Unravelling an allochthonous, subaqueously-deposited volcanic-epiclastic to subaerial andesitic lava assemblage in Hong Kong: Age, stratigraphy and provenance studies of the Middle Jurassic Tuen Mun Formation

R.J. Sewell [1]*, K.W.F. So[1], D.L.K. Tang[1], A.Carter,[2]

[1]*Hong Kong Geological Survey, Geotechnical Engineering Office, Civil Engineering and Development Department, 101 Princess Margaret Road, Kowloon, Hong Kong, China*

[2]*Department of Earth and Planetary Sciences, Birkbeck, University of London, Malet Street, London, WC1E 7HX, UK*

**Corresponding author (email: jsewell@cedd.gov.hk)*

Abstract: The Middle Jurassic Tuen Mun Formation, Hong Kong, is a fault-bounded block of rare andesitic and related rocks that preserve a snapshot of the developing southeast China continental arc system during the late Mesozoic. The depositional setting is considered to have been dominated by an emergent andesitic volcanic massif, transitioning into a fluvial-dominated volcanic plain, and then to an offshore marine environment. The youngest (<190 Ma) LA-ICP-MS U–Pb detrital zircon ages obtained from the three packages define a coherent group (n = 399; MSWD = 3.0) suggesting a maximum depositional age of 169.5 ± 0.3 Ma. The dominance of large euhedral and concentrically-zoned zircons reflects a common volcanic provenance. Hf isotope data ($\varepsilon_{Hf}(t)$ = 0 to -11) on the youngest representative zircon grains imply derivation of magmas from dominantly recycled crustal sources. The detrital zircon age signatures and Hf isotope data from analysed samples show no indication of magmatic interaction with adjacent late Palaeozoic and Early to Middle Jurassic sedimentary rocks, or Middle Jurassic to Early Cretaceous magmatic rocks of Hong Kong. Combined with structural, zircon age and isotope data, the Tuen Mun Formation is interpreted to be an allochthonous block, emplaced in the Hong Kong region during the late Middle Jurassic.

Supplementary Material: Full dataset of U–Pb dating and Hf isotope analysis of detrital zircons, stratigraphic drillhole logs, and description of the terminology used in this paper, are available at www.geolsoc.org.uk/SUPXXXX

Despite the considerable research carried out on Middle Jurassic to Early Cretaceous intermediate to silicic volcanic and intrusive rocks in the Hong Kong Special Administrative Region, China, (hereafter Hong Kong) (e.g. Sewell *et al.* 2000 and references therein; Campbell *et al.* 2007; Sewell *et al.* 2012) and mainland southeast China (e.g. Guo *et al.* 2012; Huang *et al.* 2012), relatively little is known about the age, stratigraphy and provenance of rarely exposed andesite and related rocks (e.g. BGMRPG 1988; Zhen 1988; Guo *et al.* 2012; Li *et al.* 2014) that stratigraphically predate them. In Hong Kong, these andesitic rocks are thought to represent an expression of continental arc-related mafic to intermediate magmatism associated with subduction of the palaeo-Pacific plate beneath the southeast China continental margin (Langford *et al.* 1989; Campbell & Sewell 1997; Sewell *et al.* 2000; Li *et al.* 2009; Li *et al.* 2014). The scarcity of such rocks in the coastal region of southeast China has led some workers (e.g. Xue *et al.* 1996; Mao *et al.* 2014) to question whether a Late Mesozoic Andean-type continental margin ever existed. Thus, the andesitic sequence in Hong Kong provides an important opportunity to examine the developing continental arc system, yielding the most direct evidence for the existence of Late Mesozoic mafic to intermediate juvenile continental arc-related crust along the southeast China margin. Study of the sequence can also lead to improved understanding of the interrelationships between marginal basin sedimentation and evolving arc tectonics (e.g. Kokelaar & Howells 1984 and references therein; White & Busby-Spera 1987; Aitchison & Landis 1990; Song & Lo 2002). However, the complexity of geological processes in such subaerial and submarine environments, and considerable lateral facies variations, may present challenges for classification and description of lithological assemblages.This is particularly evident where the rocks are largely concealed and have been subjected to post-emplacement deformation, metamorphism and hydrothermal alteration (e.g. White & McPhie 1996).

In order to decipher the stratigraphy of these geologically diverse successions, make sense of facies transitions, identify the source regions of lithological components and assemblages, and reconstruct the original depositional setting, a multidisciplinary approach involving detailed petrographic, mineralogical, geochronological and geochemical studies, underpinned by meticulous field work, is required. The benefits of such comprehensive study are that even on a relatively small outcrop of rarely exposed rocks, a trove of useful information can be extracted which may have important implications for understanding of the regional tectono-magmatic framework. A case study is presented here of unraveling a particularly complex andesitic succession in an urban setting, which may serve as a representative model that can be

applied elsewhere.

Tuen Mun Formation

A relatively small outcrop (26 km^2) of andesitic and related rocks is preserved in the western New Territories, Hong Kong, underlying the north-trending Tuen Mun valley (Fig. 1). These rocks constitute a fault-bounded, variably metamorphosed volcanic-related sequence, dominated by lavas and lapilli-bearing ash crystal tuffs in the upper part, and reworked tuffs and epiclastic rocks including marble clast-bearing rocks, in the lower part (Langford *et al.* 1989; Sewell *et al.* 2000). Surface exposures are, however, restricted to less than half of the outcrop area (Fig. 1), with the majority of rocks buried beneath Quaternary alluvial and marine deposits and thus only accessible from drillholes.

For over two decades there has been a controversy among geologists in Hong Kong over how to describe and interpret these rocks, which have been assigned to the Tuen Mun Formation (Langford *et al.* 1989; Sewell *et al.* 2000; Lai *et al.* 2004; Li *et al.* 2014). Whereas the classification and interpretation of lavas and lapilli-bearing ash crystal tuffs in the upper part of the formation has been relatively uncontested, the classification and interpretation of tuffaceous and epiclastic rocks, particularly marble clast-bearing rocks, in the lower part of the formation has been open to debate (e.g. Lai *et al.* 2004; Tang 2007; Lai & Chan 2012; Lai 2013; Li *et al.* 2014; Lai 2016; So & Sewell 2017). Accordingly, in this paper we integrate the findings of earlier workers (e.g. Darigo 1990; Frost 1992; Lai *et al.* 2004; Tang, 2007) within a detailed review of the age, stratigraphy and provenance of the Tuen Mun Formation. We present the results of 955 laser ablation inductively coupled mass spectrometry (LA-ICP-MS) U–Pb detrital zircon ages and Hf isotope analyses from a suite of samples taken from a broad range of lithologies. We propose a revised stratigraphy and new depositional model which explains the variety of lithofacies assemblages present, and offers insights into the complex palaeoenvironments associated with andesitic volcanism. We discuss the wider regional context, particularly in relation to the developing arc system along the southeast China continental margin.

Regional Geological Setting

Intermediate to silicic volcanic and plutonic rocks belonging to the Early Jurassic to Late Cretaceous Southeast China Magmatic Belt (Davis *et al.* 2001; Dong *et al.* 2015) are exposed across a broad (400–km-wide) NE-trending area of southeast China (Fig.

1). Numerous tectonic models have been proposed to explain this widespread igneous activity including, palaeo-Pacific plate subduction beneath East Asia (Jahn *et al.* 1976; Zhou *et al.* 2006; Li & Li 2007; Shi & Li 2012), intraplate rifting and extension (Gilder *et al.* 1996; Shu *et al.* 2009; Wang & Shu 2012; Huang *et al.* 2013), thin-skinned continental orogenesis (Hsü *et al*. 1990), and post-orogenic magmatism (Chen *et al.* 2008). However, the general consensus considers that an Andean-type convergent margin existed for a period of ca. 100 million years in the Late Mesozoic during which the palaeo-Pacific plate (or Izanagi Plate) was subducted beneath the southeast China continental margin (Eurasian Plate).

Tentative correlations with the geology of Shenzhen, Guangdong Province, immediately to the north of Hong Kong (Tang 2007), suggest that lithofacies of the Tuen Mun Formation may have counterparts in the Jilingwan Formation and possibly, the underlying Tangxia Formation (Zhen 1988). These rocks are described as comprising an upper section of andesitic tuff, lava, and dacite, and a lower section of andesitic tuff breccia, tuffaceous sandy conglomerate, sandstone, siltstone, and mudstone (Zhen, 1988; Compiling Group of Shenzhen Geology, 2009). Elsewhere in Guangdong Province, outcrops of Middle Jurassic andesitic rocks have only been rarely reported (e.g. Guo et al. 2012).

Over 80% of the exposed rocks in Hong Kong comprise intermediate to silicic granitic and volcanic rocks belonging to four main periods of Middle Jurassic to Early Cretaceous (164–141 Ma) magmatic activity (Sewell *et al.* 2000; Sewell *et al.* 2012). Among the volcanic rocks, dacitic to rhyolitic ash-flow tuffs predominate, with subordinate tuffaceous sedimentary rocks, and lavas. Monzogranite and subordinate granodiorite intrusions, along with a small amount of quartz monzonite, comprise the plutonic equivalents of the volcanic rocks. All of these rocks have been precisely dated by zircon isotope dilution thermal ionization mass spectrometry (ID-TIMS) U–Pb methods (Davis *et al.* 1997; Campbell *et al.* 2007; Sewell *et al.* 2012) and their whole-rock geochemistry (Sewell *et al.* 1992; Sewell & Campbell 1997) reflects a calc-alkaline, subduction-related signature.

Exposures of andesitic lava and tuff in the western foothills of the southern Tuen Mun valley indicate that at least part of the Tuen Mun Formation comprises primary magmatic rocks (Langford *et al.* 1989). Elsewhere in the Tuen Mun valley, the andesitic character of the formation is not always apparent, due in part to dynamic metamorphism of the rocks, hydrothermal alteration, and changes in lithofacies characteristics from south to north (Darigo 1989). Granites either side of the Tuen

Mun Valley (Fig. 1), precisely dated at 159.6 ± 0.5 Ma and 159.3 ± 0.3 Ma (Davis *et al.* 1997), have intrusive contacts with the Tuen Mun Formation (Langford *et al.* 1989).

Carboniferous sedimentary rocks and Early to Middle Jurassic sedimentary rocks are exposed east of exposures of the Tuen Mun Formation in the western northwest New Territories of Hong Kong (Fig. 1). These rocks have undergone low grade regional metamorphism (to greenschist facies), and locally have been subjected to dynamic metamorphism along major shear zones (Langford *et al.* 1989; Tang 2007).

Previous Work

Allen & Stephens (1971) described the rocks of the lower Tuen Mun valley as comprising mainly sedimentary and water-lain volcanic rocks. However, the first report of andesitic rocks from the Tuen Mun valley was by Langford et al. (1989) (Table 1). The rocks were described as andesite lavas, with subordinate interbedded lapilli-bearing ash flow crystal tuffs, tuffaceous sedimentary rocks and tuff-breccias, and assigned to the Tuen Mun Formation. The formation underlies much of the Tuen Mun valley with exposures of andesites and tuffs restricted to the southwestern and southern Tuen Mun valley, respectively. Langford *et al.* (1989) considered the western margin of the Tuen Mun Formation to be in fault contact with granite and Carboniferous metasedimentary rocks whereas the eastern margin to be in fault contact with Carboniferous rocks featuring buried marble karst (Ha *et al.* 1981). Much of the formation was reported to be foliated due to dynamic metamorphism associated with a broad complex shear belt (Lo Wu – Tuen Mun Fault Zone; Burnett & Lai 1985). A separate unit of dominantly sedimentary rocks exposed in the western foothills of the southern Tuen Mun valley was assigned to the Tsing Shan Formation (Table 1; Langford *et al.* 1989). These rocks were observed to dip steeply (70°) to the west and were considered to be overturned based on textural and structural observations (Langford *et al.* 1989). The Tsing Shan Formation was tentatively inferred to lie stratigraphically below the Tuen Mun Formation although the contact was not observed. Additionally, a small outcrop of metasedimentary rocks exposed in the northwestern corner of the Tuen Mun valley was assigned to the Carboniferous Lok Ma Chau Formation.

Darigo (1990) identified a strongly mylonitised, marble clast-bearing breccia unit from drillholes in the central Tuen Mun valley along the eastern faulted margin of the Tuen Mun Formation. These rocks were assigned to a member unit (Tin Shui Wai

Member) of the Tuen Mun Formation (Table 1). The Tin Shui Wai Member was tentatively interpreted to be a block-bearing andesitic tuff associated with a vent complex in the south ("vent breccia model"), while in the north, it was considered to be a distal-related volcanic-sedimentary facies (Darigo 1990; Frost 1992). In 2000, the term Tsing Shan Formation was abandoned, and the revised Tuen Mun Formation was considered to comprise mainly andesite lava, with interbedded ash flow tuff, metasedimentary rocks and marble clast-bearing tuff-breccia (Table 1; Sewell *et al.* 2000).

Tang (2007) carried out a detailed study on the metamorphosed sedimentary and volcanic rocks of the Tuen Mun Formation and was first to recognize "peperite" (after White *et al.* 2000) in some drillholes. This comprised evidence for andesite magma-sediment mingling interpreted to reflect *in situ* disintegration of semi-consolidated, typically wet, sediments due to injection of andesite dykes and sills. Volcanic lithofacies were considered to have been deposited by a variety of processes, including primary volcanic activities, and reworking of pyroclastic-rich deposits. Epiclastic deposits were interpreted to have been generated by normal sedimentary processes, such as fluvial processes or debris flows (Tang 2007).

The "vent breccia model" for the origin of marble clast-bearing breccia (Tin Shui Wai Member) in the Tuen Mun Formation proposed by earlier workers (e.g. Darigo 1990; Frost 1992) was later expanded to encompass all lithologies within the lower part of the formation following apparent recognition of *in situ* diatreme-like palaeo-volcanic plugs in the western Tuen Mun valley (Lai *et al.* 2004; Lai & Chan 2012). The range in compositions from andesite to dacite and minor rhyolite in the fine matrix surrounding the entrained xenoliths was considered to result from variable degrees of assimilation (i.e. physical mixing) between country rock fragments (principally marble and sandstone clasts, with minor volcanic clasts) and the intruding andesite magma (Li *et al.* 2014). The marble and sandstone clasts were inferred to have been derived from neighbouring Carboniferous rocks (San Tin Group).

Early attempts to determine the magmatic age of the volcanic rocks by radiometric methods proved largely unsuccessful, due mainly to the absence of zircon in the andesites and metamorphic overprinting. Nevertheless, a small fragment of andesite and a single amphibole crystal returned ^{40}Ar–^{39}Ar ages of 181 ± 3 Ma and 182 ± 35 Ma respectively, suggesting the rocks were late Early Jurassic in age (Evensen & York 1998). Based on U–Pb dating of eleven zircon grains from one sample in a drillhole from the lower Tuen Mun valley, Li *et al.* (2014) concluded that Tuen Mun Formation

lava had a crystallization age of 163.4 ± 0.9 Ma and was, therefore, coeval with the early phase of Middle Jurassic intermediate to silicic magmatism (Davis *et al.* 1997).

Analytical Methods

Detrital zircon U–Pb dating was carried out on seven samples from separate locations within the Tuen Mun valley, including newly identified member units proposed under this study (see below), in order to determine the maximum depositional age and provenance characteristics of the rocks. Four samples (HK13455–HK13458) came from surface outcrops, while the remaining samples (HK12821, HK13081 and HK13451) came from drillholes. One sample (HK13457) was selected for Hf isotope analysis to characterize the crustal source materials. Field-checking of selected rock exposures was carried out to verify stratigraphic observations from drillholes. A new solid geology map for the Tuen Mun valley showing the locations of dated samples and reference drillholes is presented in Figure 1. Description and location details of analysed samples are given in Table 2. Summary stratigraphic sections from key reference drillholes are shown in Figure 2.

Zircon LA-ICP-MS U–Pb analysis

Detrital U–Pb zircon analysis was carried out by laser ablation inductively coupled mass spectrometry (LA-ICP-MS) at the London Geochronology Centre based in University College London. Heavy minerals were separated from bulk sediment samples using standard density liquid and magnetic separation procedures. Zircon-enriched extracts were mounted in hard epoxy resin on glass slides and polished for analysis. Polished grain mounts were Cathodoluminescence (CL) imaged to help understand the growth stages of each zircon, enable detection of inherited cores (xenocrysts) and identify metamorphic zircon. Samples were analysed on an Agilent 7700 quadrupole-based inductively coupled plasma mass spectrometer (ICP-MS) coupled to a New Wave Research UP193FX 193 nm excimer laser following the methodology of Jackson *et al.* (2004). Typical laser spot sizes of 25 μm were used with a 7–10 Hz repetition rate and a fluence of 2.5 J/cm^2. Background measurement before ablation lasted 15 seconds and laser ablation dwell time was 25 seconds.

Repeated measurements of external zircon standard Plešovice which has a TIMS reference age 337.13 ± 0.37 Ma (Sláma, J. *et al.* 2008) was used to correct for instrumental mass bias and depth-dependent inter-element fractionation of Pb, Th and

U. Standard errors on isotope ratios and ages include the standard deviation of $^{206}Pb/^{238}U$ ages of the Plešovice standard zircon. Time-resolved signals that record isotopic ratios with depth in each crystal were processed using GLITTER 4.5, data reduction software, developed by the ARC National Key Centre for Geochemical Evolution and Metallogeny of Continents (GEMOC) at Macquarie University and CSIRO Exploration and Mining. Processing enabled filtering to remove spurious signals owing to overgrowth boundaries, weathering, inclusions, or fractures and ages were rejected if discordance exceeded 15%. Ages were calculated using the $^{206}U/^{238}Pb$ ratios for samples dated as <1.1 Ga, and the $^{207}U/^{206}Pb$ ratios was used for older grains. Discordance was determine using ($^{207}Pb/^{235}U$ - $^{206}Pb/^{238}U$) / $^{206}Pb/^{238}U$) and similar for $^{207}U/^{206}Pb$ ages. Data in this study were plotted using a statistically more robust alternative to the probability density plots known as the Kernel Density Estimator or KDE (Vermeesch, 2012). Probability density plots are unsuited to U–Pb datasets where single grain errors are typically < 5% because they produce noisy results that obscure the underlying probability distribution.

Zircon Hafnium isotope analysis

Hafnium isotope analyses were carried out on the same grains in a duplicate sample (HK13457a) analysed for U–Pb dating. Hafnium isotope analyses were performed at the NERC Isotope Geosciences Laboratory (NIGL) on a Neptune Plus multi-collector ICP-MS coupled to a New Wave Research UP193FX 193 nm excimer laser ablation system. A static spot ablation protocol was employed utilizing a 25μm beam and a 7 Hz laser pulse repetition rate. A fluence of 6.5 J/cm^2 and ablation time of 40 seconds resulted in total Hf signals for the Mud Tank reference zircon averaging 7V and combined uncertainties of 1.3 **ε**Hf units (2σ) assuming an age uncertainty of 1 Ma (1σ). Zircon standard 91500 was used to normalise the $^{176}Lu/^{177}Hf$ ratio assuming a value of 0.000311 (Woodhead and Hergt, 2005). Analytical uncertainties include the standard error of the mean of the analysis and the excess variance of the primary ablation reference material. εHf values were calculated using a ^{176}Lu decay constant of 1.865 x $10^{-11}y^{-1}$ (Scherer *et al.*, 2001), the present-day chondritic $^{176}Lu/^{177}Hf$ value of 0.0334 and $^{176}Hf/^{177}Hf$ ratio of 0.282785 ± 11 (2σ) (Bouvier, *et al.*, 2008).

Results

Detrital zircon age spectra for the seven analysed samples are shown in Figure 3. The age spectra are almost identical with a dominant population at 169 Ma and minor peaks at 440 Ma, 760 Ma, 920 Ma, 1860 Ma and 2490 Ma. Thus, the detrital zircon

ages suggest the rocks of the Tuen Mun Formation have a common provenance which helps to confirm their stratigraphic grouping. The youngest (<190 Ma) coherent age group (399 grains, MSWD = 3.0) from all seven samples converges at 169.5 ± 0.3 Ma. Representative CL images (Fig. 4) reveal that the youngest ages are from euhedral magmatic zircons implying derivation from volcanic terrain of Middle Jurassic age. The over 200 grain ages that define the mean age at 169 Ma may contain a range of magmatic events but it is not possible to discern this owing to overlapping error bars. The range of older ages aligns with an early Palaeozoic orogenic belt in South China region (Yao *et al.* 2011; Yao *et al.* 2014; Wang *et al.* 2015) that has traditionally been called the "Caledonian orogen" in the Chinese literature. The event spans to Ordovician to early Devonian and includes widespread metamorphism and magmatism between 450–420 Ma. More recent work has attempted to steer away from the European terminology by naming the event as the Wuyi-Yunkai orogeny (e.g. Li *et al.*, 2010).

With regard to Hf isotopes in zircon, as the age spectra are almost identical (Fig. 3), data from a single analysed sample, HK13457a, are considered to be representative of the Tuen Mun Formation as a whole. The negative $\varepsilon_{Hf}(t)$ values (0 to -11) for the youngest zircons (< 190 Ma) suggest that the rocks have a dominantly recycled crustal source origin (Fig. 5).

Stratigraphy

Proposed Nomenclature

So & Sewell (2017) identified four main lithotypes: andesites, including lava and intrusions; pyroclastic rocks, including tuff and tuff-breccia; mixed pyroclastic-epiclastic rocks; and epiclastic rocks. The four lithotypes are here assigned to three member units; namely the Tuen Mun Andesite, Tin Shui Wai, and Siu Hang Tsuen, respectively, based on compositional and lithofacies assemblages (Table 3).

The Tin Shui Wai Member is stratigraphically the oldest unit and occurs almost always as subcrops in drillholes along the eastern margin of the Tuen Mun valley. This unit is conformably overlain by the Siu Hang Tsuen Member, which is mainly exposed along the western foothills of the Tuen Mun valley. The Tuen Mun Andesite Member conformably overlies the Siu Hang Tsuen Member and is exposed mainly in the southern and southwestern parts of the Tuen Mun valley. Representative field photographs of the main lithologies are show in Figures 6a–f, with drillhole examples

shown in Figures 7a–h and thin section examples given in Figures 8a–f. Details of the three members are described in the following sections.

Tin Shui Wai Member (modified after Darigo 1990)

The Tin Shui Wai Member is defined as a north-trending subcrop of moderately westward dipping dominantly monomictic tuffaceous–epiclastic rocks along the eastern margin of the Tuen Mun valley extending from Tin Shui Wai in the north to Castle Peak Bay in the south (Fig. 1). The member was originally described as "an interbedded sequence of volcaniclastic rocks, including tuff-breccia, fine to coarse andesitic tuff and tuffite, tuffaceous siltstone, lapilli tuff and andesitic conglomerate" (Darigo 1990). The type drillhole is here defined as Drillhole TH1 (Fig. 2) which is located on the southern outskirts of Tin Shui Wai (Fig. 1). The member has an estimated minimum thickness of 300 m based on *c.* 40° westerly dip of the bedding and known limits of subcrop from drillholes in the central Tuen Mun valley.

Dominant Lithofacies. The most distinctive lithofacies is monomictic, marble clast-bearing, breccia/sandstone/siltstone, and may be tuffaceous or epiclastic. The tuffaceous variety occurs as matrix-supported, marble clast-bearing tuffaceous breccia layers, interbedded with andesitic lapilli-bearing tuffaceous sandstone and siltstone (Fig. 6a). These rocks are largely restricted to an elongated zone along the eastern faulted margin of the Tuen Mun Formation (Fig. 1), which is generally less than 1 km-wide in the centre of the valley but narrows to approximately 200 m in the north and south. Rocks adjacent to the eastern boundary fault are strongly dynamically metamorphosed to mylonite and ultramylonite featuring attenuated marble clasts, and making identification of original mineralogy in the matrix impossible. However, westwards from this boundary fault, particularly in the central part of the valley, drillholes have recorded less deformed sequences which reveal that the matrix to these breccia-conglomerate layers is tuffaceous with euhedral andesine phenocrysts and titanomagnetite (Fig. 8a).

The andesitic tuffaceous component of the Tin Shui Wai Member diminishes from the central Tuen Mun valley to the northern Tuen Mun valley so that in the Tin Shui Wai area, the lithofacies is dominated by epiclastic monomictic, marble clast-bearing breccia, sandstone and siltstone. Close examination of drillhole cores and thin sections from these less deformed sequences reveal fining upward cycles (1.5–5 m thick) from marble clast-bearing breccia-conglomerate or coarse sandstone to fine siltstone (TH1; Fig. 2). The fine siltstone layers also show an abundance of quartz in

the matrix and contacts with marble clasts are sharp and show little sign of alteration (Fig. 8b). Intercalated sandstone layers are commonly calcareous, particularly in the northern part of the Tuen Mun valley.

Marble clast-bearing layers in which the proportion of angular marble clasts exceeds 50%, are classified as marble breccia (Fig. 7c). Owing to their strongly deformed, clast-supported character, these breccia layers may superficially resemble foliated impure marble. However, when subjected to weathering, the dissolved marble clasts leave behind a skeletal residuum composed dominantly of the residual quartz grains (Fig. 7c; inset).

Subordinate lithofacies. In the central Tuen Mun valley, the monomictic marble clast-bearing units are sometimes intruded by andesite dykes and sills (Fig. 7a) and are characterized by the development of monomictic, andesite-breccia peperite. In some drillholes, there is also evidence for mingling of andesitic magma with unconsolidated monomictic marble clast-bearing sediments, leading to considerable hydrothermal alteration and contact metamorphism effects (Fig. 7d). Skarn minerals, such as garnet and epidote, are common alteration products in these rocks due to reaction between hot magma and marble clasts. Mingling of andesite magma and wet sediments, with or without marble clasts or a tuffaceous component, produces an andesite-sandstone peperite. This subordinate lithofacies variant is found mainly in the central Tuen Mun valley, but may occur in all three member units of the Tuen Mun Formation.

Siu Hang Tsuen Member (new)

The newly proposed Siu Hang Tsuen Member is the name given for dominantly polymictic tuffaceous–epiclastic rocks forming a north-trending outcrop exposed mainly on the western foothills of Tuen Mun valley (Fig. 1). A significant portion of the member forms a subcrop in the central part of the Tuen Mun valley. The member is named after the location of the type drillhole (BH-3; Fig. 1) which is in the central Tuen Mun valley. It has an estimated minimum thickness of 1100 m. The base of the member is gradational and conformable with the underlying Tin Shui Wai Member as shown in several drillholes (e.g. HSK-1; Fig. 1). Overall, the tuffaceous (andesitic) component of the matrix is gradually replaced by a quartz-dominated component from south to north.

Dominant Lithofacies. Polymictic, conglomerate/sandstone/siltstone with or without

marble clasts is the dominant lithofacies and may be tuffaceous or epiclastic. The tuffaceous lithofacies is most commonly observed in the central and southern Tuen Mun valley. Outcrops on the western foothills typically comprise an interbedded sequence of massive, clast-supported, poorly sorted, boulder to cobble, tuffaceous, polymictic breccia-conglomerate and normally graded, clast- to matrix-supported, poorly to moderately sorted, cobble to pebble, polymictic breccia-conglomerate grading upward to well sorted coarse to fine quartz sandstone and siltstone. Clast compositions in the conglomerate include andesite lava, coarse ash tuff, marble, quartz sandstone, and feldsparphyric rhyolite (Fig. 6d). The younging direction identified from drillholes (e.g. 1983D; Fig. 2) and outcrops (Langford *et al.* 1989) along the western foothills reveal that the sequence is overturned and polymictic conglomerates are interbedded with tuffaceous sandstone and siltstone units. The epiclastic unit is mainly observed in central and northern Tuen Mun valley. At the type drillhole (BH-3; Figs 2, 7f), a typical younging upward, cyclical unit (up to 5.5 m) is observed at a core depth of 33.17 m. The base of this unit consists of clast-supported, cobble to pebble, polymictic, breccia-conglomerate in sharp contact with underlying black siltstone. A small block of polymictic breccia-conglomerate occurs as an isolated raft in the siltstone a few centimeters below the main contact. The clast-supported, polymictic, breccia-conglomerate is massive for about 3 m before transitioning gradually to matrix-supported breccia-conglomerate with layers of coarse sandstone containing isolated clasts becoming more common. Matrix-supported breccia-conglomerate (over 2.5 m thick) fines upward to dominantly coarse sandstone with isolated clasts. The coarse sandstone is then overlain sharply, but conformably, by black siltstone, with some siltstone intermingling with the top of the coarse sandstone unit. The black siltstone is up to 4 m thick and is overlain by another cyclic unit of clast-supported, polymictic, breccia-conglomerate, sandstone and siltstone. In the northern Tuen Mun valley (e.g. BGS15; Fig. 2), polymictic breccia-conglomerate is interbedded with massive to normally graded, well sorted, coarse to fine quartz sandstone and siltstone. Exposures of polymictic conglomerate with intercalated laminated sandstone and siltstone in the western central Tuen Mun valley display load structures (Fig. 6a) and weakly developed cross-bedding (Fig. 6b).

Subordinate lithofacies. Polymictic, andesite-conglomerate peperite, with or without marble clasts are sporadically observed in central and southern Tuen Mun valley. This lithofacies is associated with intrusion of andesitic dykes and sills. Drillholes (e.g. Fig. 7e) reveal evidence for magma injection into wet semi-consolidated sediment, causing intensive brecciation accompanied by development of reaction rims around marble

clasts, set within a hydrothermally altered matrix (Fig. 7e; inset). Field exposures of this lithofacies (Fig. 6c) show evidence for injection of fluidal andesite magma into unconsolidated breccia-conglomerate as revealed by billowed chilled margins and baking of the surrounding sediment. Entrained patches of breccia-conglomerate within the intruding magma (Fig. 6c) display incipient disaggregation indicating the unconsolidated character of the host matrix.

Tuen Mun Andesite Member (modified after Langford et al. 1989)

The modified Tuen Mun Andesite Member is the name given for the andesite lava, lapilli-bearing ash-flow crystal tuff, and tuffaceous sandstone and siltstone components of the Tuen Mun Formation (Langford *et al.* 1989) which crop out in the southern Tuen Mun valley (Fig. 1). These rocks are considered to represent the principal magmatic component of the formation and their type locality is designated to be exposures of andesite in rock slopes cut into the western foothills overlooking Tuen Mun (Langford *et al.* 1989).

Dominant Lithofacies. Andesite lava, autobreccia, and andesitic lapilli-bearing ash-flow crystal tuff belonging to this lithofacies are variably mylonitised making it difficult to identify individual flow units. However, in the foothills west of Tuen Mun, slightly less deformed lavas display a uniform porphyritic texture comprising euhedral microphenocrysts of andesine and amphibole, set in a pilotaxitic groundmass of feldspar, amphibole and biotite (Fig. 8e). Individual flow units, up to 4 m thick, are separated by zones of autobreccia or layers of crystal-rich ash flow tuff (Figs 6e, 7g). Some zones of complete andesite lava brecciation are also apparent in drillholes (Fig. 7h). Andesitic lapilli-bearing ash-flow crystal tuffs show variable crystal contents (Fig. 8f) and frequently host block and lapilli-sized andesite lava fragments (Fig. 6f).

Subordinate Lithofacies. Reworked crystal-rich tuffaceous sandstone with andesitic composition is encountered in drillholes in the southern Tuen Mun valley (e.g. PD-20; Fig. 2). These tuffaceous sandstone layers are up to 10 m thick, with feldspar crystal lapilli within the sandstone generally concentrated in zones, and less commonly, sparsely but evenly distributed. Near the top of each layer, the sandstone grades upward into siltstone containing sporadic crystals of feldspar, before being overlain by the succeeding sandstone unit. The crystal-rich sandstone layers are sometimes separated by block-bearing andesitic tuff units containing fragments of andesite lava, and rarely, tuffaceous sandstone.

Discussion

Detrital Zircon Age and Provenance

Compared with the younger LA-ICP-MS U–Pb zircon age of 163.4 ± 0.9 Ma obtained by Li *et al.* (2014) based on 11 grains from one tuffaceous sample, the slightly older maximum depositional age for the Tuen Mun Formation (169.5 ± 0.3 Ma) obtained in our study is considered more representative and reliable. This new age is based on an average of 117 dated detrital zircon grains from seven analysed samples collected from a range of lithologies over the entire outcrop area (Fig. 1). The euhedral shape and abundant large, fresh zircons (Fig. 4), suggests the zircon populations are of magmatic origin. The minimum depositional age for the Tuen Mun Formation is constrained by structural and stratigraphic relationships of the adjacent intermediate to silicic volcanic rocks which have been precisely-dated at 164.5 ± 0.1 Ma (Davis *et al.* 1997). There is no obvious geochemical link between the Tuen Mun Formation and major Middle Jurassic to Early Cretaceous intermediate to silicic magmatic suites of Hong Kong (Sewell & Campbell, 1997).

Cawood *et al.* (2012) proposed a model diagram which plots cumulative proportion curves of detrital zircon age data against the difference between the zircon crystallization age and depositional age (CA-DA) to help constrain tectonic setting. Three tectonic settings are portrayed: convergent, collisional, and extensional basins. Convergent margin basins (e.g forearc and trench) are considered to have a high proportion of detrital zircons with ages close to the depositional age of the sediment. Collisional basins (e.g. foreland basins) have only a minor (<10%) proportion of detrital zircon ages approximating the depositional age of the sediment, but a major proportion (10–50%) of grains with ages within 150 Ma of the depositional age. Extensional basins are characterized by a dominance of very old zircons with less than 5% of grains having ages within 150 Ma of the depositional age. Using a minimum depositional age of 164.5 ± 0.1 Ma for the Tuen Mun Formation, and plotting the cumulative proportion curves on the model diagram of Cawood *et al.* (2012) (Fig. 9), the youngest 30% of zircons have less than 100 Ma CA-DA suggesting that the Tuen Mun Formation zircons have been deposited in a convergent margin forearc setting.

Previous models have suggested that the sandstone and marble clasts within the formation originated from late Palaeozoic (San Tin Group) basement lithologies entrained within andesite volcano edifices (“vent breccia model”) (Lai & Chan 2012).

It has been proposed (Li *et al.* 2014) that the compositional variation from intermediate to silicic compositions observed in whole-rock geochemistry is due in part to processes of combined assimilation and fractional crystallization (AFC) of these xenolithic materials. However, the detrital zircon age spectra obtained in our study demonstrates that there is virtually no zircon contamination from the late Palaeozoic rocks which typically have population peaks at 440 Ma, 800–1000 Ma and 2500 Ma (Sewell *et al.* 2016; Fig. 3). Although the detrital zircon age spectra for the Tuen Mun Formation lithologies show slightly closer affinity to adjacent Early to Middle Jurassic sandstones (e.g. 1860 Ma peak; Sewell *et al.* 2016), there are also major differences, such as the absence of a 236 Ma peak which is ubiquitous among Early to Middle Jurassic sedimentary rocks. Differences among these age spectra are emphasized on a multidimensional scaling (MDS) map that displays Kolomogorov-Smirnov distances (Vermeesch 2013) in visual form (Fig. 10). The map confirms that the Tuen Mun Formation detrital zircon age spectra are distinct from adjacent groups of rocks. Likewise, the Hf isotope data from the Tuen Mun Formation show marked dissimilarities with data from adjacent Carboniferous and Early to Middle Jurassic rocks (Fig. 5), which exhibit mixed juvenile and recycled crustal sources as compared to a dominantly recycled crustal component. From these observations, we infer that there has been little or no contamination with the Tuen Mun Formation from adjacent rock units.

Previous high precision ID-TIMS U–Pb zircon dating of the adjacent Middle Jurassic (164.5 ± 0.1 Ma) Tsuen Wan Volcanic Group and Lamma Suite granites in Hong Kong have yielded zircon inheritance ages of 713 ± 61 Ma, 1134 ± 64 Ma, 1872 ± 3 Ma, 2022 ± 2 Ma and 2719 ± 4 Ma in five volcanic and granitic samples (Davis *et al.* 1997; Campbell *et al.* 2007). These ages contrast markedly with the peaks of detrital zircon ages observed in the Tuen Mun Formation (Fig. 3). Importantly, no inherited grains of magmatic (169.5 ± 0.3 Ma) zircons from the Tuen Mun Formation have been identified in these nearby volcanic and plutonic rocks. From these observations, we infer there has been no recycling of the Tuen Mun Formation rocks in the subsequent intermediate to silicic Middle Jurassic (164.5 ± 0.1 Ma) magmatic rocks of Hong Kong.

The abundant zircon in all main lithofacies of the Tuen Mun Formation, except andesite lava and tuff, suggests a contribution from intermediate to silicic volcanic sources. Although no outcrops of these magmatic rocks are known in the Tuen Mun Formation, feldsparphyric rhyolite and quartz-rich coarse ash crystal tuff clasts are commonly observed in the polymictic conglomerates of the Siu Hang Tsuen Member,

571 especially in the southern Tuen Mun valley (Figs 6d, 8b), suggesting input from a
572 nearby dacitic to rhyolitic source that might have been exposed outside Hong Kong
573 during the depositional period. Dacite lava of Early to Middle Jurassic age
574 (Jinlingwan Formation) has been reported from Shenzhen, Guangdong Province,
575 immediately to the north of Hong Kong (UPLRCSM 2007).
576
577 *Structure and Metamorphism*
578
579 Evidence for mylonitisation, particularly along the eastern portion of the Tuen Mun
580 Formation (Tang 2007), suggests that the formation has been tectonically juxtaposed
581 with adjacent Carboniferous and Early to Middle Jurassic sedimentary rocks.
582 Mylonites are most strongly developed within 1 km of the East Tuen Mun Fault and
583 gradually diminish towards the west (Fig. 1). The western boundary of the Tuen Mun
584 valley is also faulted with evidence of mylonitisation. However, the boundary is in
585 part intrusive, with contact metamorphism evident as a result of granite intrusion.
586 Some workers (e.g. Langford *et al.* 1989) have suggested that the granite contact
587 along the western boundary of Tuen Mun valley may be a thrust fault coincident with
588 an intrusive contact.
589
590 Observations of overturned bedding in the southern Tuen Mun valley (Langford *et al.*
591 1989) imply that Tuen Mun Formation has been folded. In contrast to adjacent Early
592 to Middle Jurassic and Carboniferous rocks, the Tuen Mun Formation has not been
593 regionally metamorphosed to greenschist facies (Langford *et al.* 1989). The outcrop
594 pattern member units of the Tuen Mun Formation suggests an overturned syncline
595 with the NNW trending fold axis plunging to the SSE. Subsequent intrusion by
596 granite appears to have truncated the western overturned limb of the fold in the south.
597 Folds in the Tuen Mun Formation have also been reported by Langford *et al.* (1989)
598 along the western edge of the Tuen Mun valley adjacent to the boundary with the
599 granite.
600
601 Major differences in the age, stratigraphy, structure, and detrital zircon provenance
602 between the Tuen Mun Formation and adjacent rock units, together with evidence for
603 strike-slip juxtaposition, suggests that the Tuen Mun Formation likely belongs to a
604 separate tectonic block. While the origin of this tectonic block and characteristics of
605 its crustal basement are unknown, possible correlatives of the Tuen Mun Formation
606 exist in nearby Shenzhen, Guangdong Province (Tang 2007) implying that it could
607 have been derived from the north. Sewell *et al.* (2016) have recently identified the
608 existence of an exotic terrane (Tolo Terrane) in southeastern Hong Kong that is

609 considered to have accreted to the southeastern Cathaysia margin in the late Middle
610 Jurassic. Collision and accretion coincided with a major late Middle Jurassic
611 deformation event in northwestern Hong Kong characterized by thrusting, folding and
612 regional metamorphism. The maximum age of juxtaposition of the Tuen Mun
613 Formation is constrained by the timing of this deformation event which is thought to
614 have occurred between 164 and 161 Ma (Sewell *et al.* 2016). The minimum age of
615 juxtaposition is constrained by the ages of the Tsing Shan and Tai Lam granites (*c.*
616 161–159 Ma, Sewell *et al.* 2012). Thus, it is inferred that juxtaposition probably
617 coincided with a major deformation event in northwestern Hong Kong associated with
618 collision and accretion of the Tolo Terrane along the southeast China continental
619 margin (Sewell *et al.* 2016).
620
621 *Stratigraphy and Depositional Settings*
622
623 The numerous lithofacies present in the Tuen Mun Formation suggest depositional
624 settings were highly variable and complex, with both subaerial and subaqueous
625 sequences represented.
626
627 Monomictic, marble clast-bearing layers and marble breccias, with or without
628 tuffaceous components, and commonly separated by thick calcareous sandstone and
629 siltstone units, suggest deposition in a subaqueous environment principally by gravity
630 mass flows (cf. Wood & Wallace 1986). The marble breccias possibly represent
631 reworking of submarine carbonate deposits, or material derived from coastal
632 carbonate cliffs (cf. Flugel 2010). The abundance of quartz in the matrix implies a
633 near-shore terrigenous rhyolitic component, while andesitic tuffaceous material could
634 be derived from both subaerial or subaqueous sources. The occurrence of fluidal
635 peperite within marble clast-bearing breccia units, along with andesite dykes and sills,
636 implies contemporaneous submarine volcanism (Cas *et al.* 2001).
637
638 Abundant evidence for grading, rounding of clasts, cross-bedding and imbrication
639 suggests that the polymictic conglomerates and breccias of the Siu Hang Tsuen
640 Member are dominantly of epiclastic origin. Both terrestrial and subaqueous
641 depositional settings are indicated by the sedimentary structures. Cross-bedding in the
642 polymictic conglomerates implies traction–current deposition, possibly in a high
643 energy, fluvial or shoreline environment. Widespread cyclical normal grading units
644 observed in many drillholes within the Siu Hang Tsuen Member is consistent with
645 deposition from subaqueous mass movements (e.g. debris flows). Fluidal peperite
646 reflects injection of andesitic magma into wet, semi-consolidated sediments, probably

below wave base or in a fluvial (e.g. floodplain) environment.

Andesite lava flows separated by autobreccia, which are exposed in the lower Tuen Mun valley, indicate a dominantly subaerial depositional setting. Generally, these units are thick and discontinuous implying that they have infilled depressions on the flanks of a volcanic massif. Some zones of complete andesite lava brecciation may represent hyaloclastites, resulting from magma/water interaction (Fig. 6h), although no pillows have been observed. Andesitic lapilli-bearing ash-flow tuffs also imply dominantly subaerial deposition. However, the appearance of thick, crystal-rich tuffaceous sandstone units suggests that some crystal tuffs may have been redeposited as gravity flows in a subaqueous setting in which the fine ash particle size fraction had been winnowed out (cf. White & McPhie 1997). Variations in the percentage of crystals observed in some crystal-rich tuffaceous sandstone units also implies reworking of volcanic deposits rather than deposition from primary pyroclastic flows.

Regional Tectono-magmatic Implications

Although the geochemical evolution of the Tuen Mun andesites and related rocks is outside the scope of this paper, whole-rock geochemistry (e.g. Sewell & Campbell, 1997; Li *et al.* 2014) has previously revealed that these rocks possess a subduction-related signature. In this context, the Hf isotope data from the youngest zircons in this study yield important clues with respect to the crustal source region. The negative $\varepsilon_{Hf}(t)$ values indicate a significant contribution from recycled crustal materials suggesting parental magmas interacted with either subducted sediment from the downgoing slab, or continental crust, or both. Either way, the Hf isotope signatures are consistent with a continental margin subduction setting interpreted from whole-rock geochemistry. Despite close proximity to Triassic S-type and Middle Jurassic A-type granitoids (Sewell & Campbell, 1997), the zircon U–Pb age and Hf isotope data of the Tuen Mun Formation suggest that parental magmas did not interact with ancient (Archaean to palaeo-Proterozoic) continental crust which is apparent in the source regions of these neighbouring plutons (Darbyshire & Sewell, 1997). Neither do the Tuen Mun Formation zircons possess an inherited component from the crustal source regions of neighbouring late Palaeozoic and Early to Middle Jurassic sedimentary rocks. These attributes are consistent with the allochthonous character of the Tuen Mun Formation already determined from structural, stratigraphic and zircon U–Pb age considerations.

The timing of the initiation of palaeo-Pacific plate subduction along the southeast

China continental margin remains controversial. Some models suggest that subduction commenced in the Early Triassic (e.g. Li & Li, 2007) while others consider it commenced in the Late Jurassic (e.g. Zhou et al. 2006). The maximum depositional age of the Tuen Mun Formation presented in this study strongly suggests that a major pulse of andesitic magmatism along the southeast China continental margin occurred during the early Middle Jurassic. The Tuen Mun Formation andesites and related rocks possess geochemical characteristics of mature continental arcs (Sewell & Campbell, 1997; Li *et al.* 2014) and, therefore, the subduction zone setting is likely to have been well-established by the early Middle Jurassic.

The Tuen Mun Formation is an important remnant of what was once a belt of continental-arc related volcanoes and fore-arc basins that existed along the southeast China continental margin associated with palaeo-Pacific plate subduction. The scarcity of preserved Early to Middle Jurassic andesite outcrops in the present coastal area is largely due to the colossal overprint of intermediate to silicic volcano-plutonism, deformation and metamorphism that affected the region from the late Middle Jurassic to Late Cretaceous (Chen *et al.* 2008; Li *et al.* 2013; Li J.H. *et al.* 2014).

Depositional Model

Based on the available data, we propose that the Tuen Mun Formation represents a complex volcanic arc-related basin featuring a sequence dominated by an emergent andesitic volcano massif in the south, transitioning northward into a fluvial-dominated volcanic plain, and then to an offshore submarine environment (Fig. 11). The proximal facies is represented by the Tuen Mun Andesite Member and associated lithologies now exposed in the southern part of the Tuen Mun valley. These preserve the most primary magmatic characteristics of the formation. The medial facies, which is dominated by fluvial deposition, is represented by the Siu Hang Tsuen Member and the distal facies by the Tin Shui Wai Member in the central and northern part of the Tuen Mun valley. However, both the medial and distal facies possess a magmatic component in southern part of the formation. It is likely that there were andesitic intrusions in all three facies environments, although these intrusions were probably spatially associated with the emergent andesite volcano massif. Polymictic conglomerates in the Siu Hang Tsuen Member point to a variety of sediment sources, including sandstone, siltstone and rhyolite sources. These sources are likely to have been mostly from terrestrial reworking of Early to Middle Jurassic rocks exposed outside Hong Kong. By contrast, the monomictic breccias of the Tin Shui Wai

Member, probably were derived from collapse and reworking of offshore carbonate deposits, or adjacent coastal carbonate cliffs, with minor inputs from other terrestrial sedimentary sources.

Conclusions

This paper has presented the first detailed age, stratigraphic and provenance study of a group of rare andesitic and related rocks associated with the developing southeast China continental arc system during the late Mesozoic. It has highlighted the importance of systematic descriptions of variable lithologies, together with detailed stratigraphic studies and age determinations, in unraveling the origin of a complex forearc assemblage. Such sequences require meticulous consideration of all available geological data in order to reconstruct a plausible depositional model. Moreover, this study reinforces emerging evidence for a major late Middle Jurassic tectonic event along the southeast China continental margin, possibly related to collision and accretion of an exotic microcontinental fragment.

The Tuen Mun Formation consists of a dominantly andesitic sequence comprised of three member units representing contrasting depositional settings. All three members contain gradational facies transitions, and feature a common magmatic provenance with maximum depositional age of about 170 Ma. Parental magmas interacted with dominantly recycled crustal sources. An emergent andesitic massif, represented by the Tuen Mun Andesite Member, is inferred for the southern portion of the outcrop. This massif fed lava and tuff to a surrounding plain represented by the Siu Hang Tsuen Member which included a fluvial system that sourced material from an adjacent dacitic to rhyolitic terrain. Primary and secondary volcanic materials were reworked and deposited principally by gravity mass movements in a shallow offshore marine environment for the Siu Hang Tsuen Member. Collapse of offshore carbonate deposits or coastal cliffs may have periodically shed detritus in the form of monomictic mass movements to deeper offshore areas. This depositional setting is represented by the Tin Shui Wai Member. Intrusions of andesite dykes and sills into unconsolidated materials of all three member units caused local contact metamorphism and hydrothermal alteration. Subsequently, the Tuen Mun Formation was juxtaposed, possibly from the north, against Carboniferous and Early to Middle Jurassic sedimentary rocks in the Hong Kong region sometime during the late Middle Jurassic between 164 and 161 Ma. This tectonic event was accompanied by strong dynamic metamorphism and deformation along the eastern margin of the outcrop. Subsequent intrusion of granite along the western boundary of the outcrop, possibly accompanied

by thrusting, may have caused local folding and overturning, and silicification, of the Tuen Mun Formation.

We thank K C Ng and J R Ali for valuable reviews of earlier drafts. We are grateful to T. Rooney, U. Knittel, and one anonymous referee for providing constructive comments on the submitted manuscript which led to considerable improvement. RJS, KWFS, and DLKT publish with the approval of Director of Civil Engineering and Development, and Head of the Geotechnical Engineering Office, Hong Kong SAR Government.

References

Allen, P.M. & Stephens, E.A. 1971. *Report on the Geological Survey of Hong Kong, 1967–1969.* Hong Kong Government Press, Hong Kong.

Aitchison, J.C. & Landis, C.A. 1990. Sedimentology and tectonic setting of the late Permian-early Triassic Stephens Subgroup, Southland, New Zealand: an island arc-derived mass flow apron. *Sedimentary Geology*, **68,** 55–74.

Bouvier A, Vervoort J.D., & Patchett, P.J. 2008. The Lu–Hf and Sm–Nd isotopic composition of CHUR: Constraints from unequilibrated chondrites and implications for the bulk composition of terrestrial planets: *Earth and Planetary Science Letters* **273,** 48–57.

Bureau of Geology and Mineral Resources of Guangdong Province (BGMRGP) 1988a. *Regional geology of Guangdong Province*. Geological Memoirs Series, 1. (In Chinese)

Burnett, A.D. & Lai, K.W. 1985. A review of photogeological lineaments in Hong Kong. *In:* I. McFeat-Smith (ed) *Geological Aspects of Site Investigation*. Geological Society of Hong Kong Bulletin **2**, 113–131.

Campbell, S.D.G. & Sewell, R.J. 1997. Structural control and tectonic setting of Mesozoic volcanism in Hong Kong. *Journal of the Geological Society, London,* **54,** 1039–1052.

Campbell, S.D.G., Sewell, R.J., Davis, D.W. & So, A.C.T. 2007. New U–Pb age and geochemical constraints on the stratigraphy and distribution of the Lantau Volcanic Group, Hong Kong. *Journal of Asian Earth Sciences,* **31,** 139–152.

Cawood, P.A., Hawkesworth, C.J. & Dhuime, B. 2012. Detrital zircon record and tectonic setting. *Geology,* **40,** 875–878.

Chen, C.H., Lee, C.Y & Shinjo, R. 2008. Was there Jurassic paleo-Pacific subduction in South China?: Constraints from $^{40}Ar/^{39}Ar$ dating, element and Sr–Nd–Pb isotopic geochemistry of the Mesozoic basalts. *Lithos,* **106,** 83–92.

Compiling Group of Shenzhen Geology 2009. *1:50,000-scale Geological Map of Shenzhen.* Geological Publishing House, Beijing (in Chinese).

Darbyshire, D.P.F. & Sewell, R.J. 1997. Nd and Sr isotope geochemistry of plutonic rocks from Hong Kong: Implications for granite petrogenesis, regional structure and crustal evolution. *Chemical Geology,* **143,** 81–93.

Darigo, N.J. 1990. Marble-bearing Jurassic volcanics of the Western New Territories, Hong Kong. *In:* R.L. Langford, A. Hansen & R. Shaw (eds) *Karst geology in Hong Kong.* Geological Society of Hong Kong Bulletin, **4,** 49–60.

Davis, D.W., Sewell, R.J. & Campbell, S.D.G. 1997. U–Pb dating of Mesozoic igneous rocks from Hong Kong. *Journal of the Geological Society, London,* **154,** 1067–1076.

Davis, G.A., Zheng, Y.D., Wang, C., Darby, B.J., Zhang, C.H. & Gehrels, G. 2001. Mesozoic tectonic evolution of the Yanshan fold and thrust belt, with emphasis on Hebei and Liaoning Provinces, northern China. *In:* Hendrix, M.S. & Davies, G.A. (eds) *Paleozoic and Mesozoic Tectonic Evolution of Central Asia: From Continental Assembly to Intracontinental Deformation*, GSA Memoir, **194,** 171–198.

Dong, S.W., Zhang, Y.Q., Zhang, F.Q., Cui, J.J., Chen, X.H., Zhang, S.H., Maio, L.C., Li, J.H., Shi, W., Li, Z.H., Huang, S. & Li, H.L. 2015. Late Jurassic-Early Cretaceous continental convergence and intracontinental orogenesis in East Asia: A synthesis of the Yanshan Revolution. *Journal of Asian Earth Sciences*, **114,** 750–770.

Evensen, N. & York, D. 1998. *Report to Hong Kong Geological Survey on ^{40}Ar–^{39}Ar laser microprobe dating of samples of HK856.* Argon Geochronology Laboratory, Department of Physics, University of Toronto.

837 Flugel, E. 2010. *Microfacies of Carbonate Rocks: Analysis, Interpretation and*
838 *Application (2nd Edition)*. Springer-Verlag Berlin Heidelberg, 228–241.
839
840 Frost, D.V. 1989. Palaeokarst of Yuen Long, north west New Territories, Hong Kong
841 *In:* Back, B.F. (ed) *Engineering and Environmental Impacts of Sinkholes and Karst*.
842 A .A. Balkeam, Rotterdam, 239–246.
843
844 Frost, D.V. 1990. Geological structure and stratigraphy of the Yuen Long area, Hong
845 Kong. In: R.L. Langford, A. Hansen & R. Shaw (eds) *Karst geology in Hong Kong.*
846 Geological Society of Hong Kong Bulletin, **4,** 49–60.
847
848 Frost, D.V. 1992. *Geology of Yuen Long*. Hong Kong Geological Survey Sheet Report
849 No. 1, Geotechnical Engineering Office, Hong Kong Government.
850
851 Gilder, S.A., Keller, G.R., Luo, M. & Goodell, P.C. 1991. Timing and spatial
852 distribution of rifting in China. *Tectonophysics,* **197,** 225–243.
853
854 Guo, F., Fan, W., Li, C., Zhao, L., Li, H. and Yang, J. 2012. Multi-stage crust-mantle
855 interaction in SE China: Temporal, thermal and compositional constraints from
856 Mesozoic felsic volcanic rocks in eastern Guangdong-Fujian provinces. *Lithos,* **150,**
857 62–84.
858
859 Ha, T.H.C, Ng, S.K.C. & Li, Q.W. 1981. Discovery of carbonate rocks in the Yuen
860 Long area. *Hong Kong. Hong Kong Baptist College Academic Journal,* **8,** 129–131.
861
862 Hsü, K.J., Li, J., Chen, H., Wang, Q., Sun, S., & Sengör, A. 1990. Tectonics of South
863 China: Key to understanding West Pacific geology. *Tectonophysics,* **183,** 9–39.
864
865 Huang, H.Q., Li, X.H., Li, Z.X. & Li, W.X. 2013. Intraplate crustal remelting as the
866 genesis of Jurassic high-K granites in the coastal region of the Guangdong Province,
867 SE China. *Journal of Asian Earth Sciences,* **74,** 280–302.
868
869 Jackson S.E., Pearson, N.J., Griffin, W.L. & Belousova, E.A. 2004. The application of
870 laser ablation-inductively coupled plasma-mass spectrometry to in situ U–Pb zircon
871 geochronology. *Chemical Geology,* **211,** 47–69.
872
873 Jahn, B.M., Chen, P.Y. & Yen, T.P. 1976. Rb–Sr ages of granitic rocks in southeastern
874 China and their tectonic significance. *Geological Society of America Bulletin,* **86,**

763–776.

Kokelaar, B.P. & Howells, M.F. (eds) 1984. *Marginal basin geology: volcanic and associated sedimentary and tectonic processes in modern and ancient marginal basins.* Geological Society of London Special Publication **16**.

Langford, R.L., Lai, K.W., Arthurton, R.S. & Shaw, R. 1989. *Geology of the Western New Territories*. Hong Kong Geological Survey Memoir No. 3, Geotechnical Control Office, Hong Kong Government.

Lai, K.W. 2013. The characteristics and misjudgment of cavernous marble and their influence on foundation design in Hong Kong. *In: Proceedings of the HKIE Geotechnical Division 33rd Annual Seminar, Hong Kong, 217–224.*

Lai, K.W. 2016. Accurate geological data is the basis of urban development. Discussion on "Guidelines on the Description and Classification of rocks of the Tuen Mun Formation". *In: Proceedings on the Asia-pacific Forum on Mega Infrastructure and Urban Development Construction 2016. Hong Kong University of Science and Technology, 1–11.*

Lai, K.W., Chan, H.H.K., Choy, C.S.M. & Tsang, A.L.Y. 2004. The characteristics of marble clast-bearing volcanic rock and its influence on foundation in Hong Kong. *In: Proceedings of the Conference on Foundation Practice in Hong Kong, E1–E10.*

Lai, K.W. & Chan, S.H.M. 2012. New evidence of palaeovolcanic plugs in the Tuen Mun area, Hong Kong: Debate on the volcanic plug or reworked pyroclastic deposits. *In: Proceedings of the 30th Anniversary Conference of the Geological Society of Hong Kong, Hong Kong*, 69–85.

Li, L.M, Sun, M., Xing, G.F., Zhao, G.C., Zhou., M.F., Wong, J. & Chen, R. 2009. Two late Mesozoic volcanic events in Fujian Province: constraints on the tectonic evolution of southeastern China. *International Geology Review,* **51,** 216–251.

Li, Z.X., & Li, X.H. 2007. Formation of the 1300-km-wide intracontinental orogen and postorogenic magmatic province in Mesozoic South China. A flat-slab subduction model: *Geology,* **35,** 179–182.

Li, Z.X., Li, X.H., Wartho, J., Clark, C., Li, W.X., Zhang, C.L., & Bao, C. 2010.

913 Magmatic and metamorphic events during the early Paleozoic Wuyi-Yunkai orogeny,
914 southeastern South China: New age constraints and pressure-temperature conditions:
915 *GSA Bulletin* **122,** 772–793.
916
917 Li, J.H., Zhang, Y.Q., Dong, S.W. & Johnston, S.T. 2014. Cretaceous tectonic
918 evolution of South China: A preliminary systhesis. *Earth-Science Reviews*, **134,**
919 98–136.
920
921 Li. Y.H., Zhou, M.F., Lai, K.W., Chan, L.S. & Chen, W.T. 2014. Geochemical and
922 geochronological constraints on Late Jurassic volcanic rocks at Tuen Mun, Hong
923 Kong, with implications for the Palaeo-Pacific subduction. *International Geology*
924 *Review.* **56**, 408–429. http://dx.doi.org/10.1080/00206814.2013.873355
925
926 Ludwig, K.R., 2001, Squid 1.02: A Users Manual rev. 20 June 2001. Berkeley
927 Geochronology Centre Special Publication No.2, 19 pp., Berkeley Geochronology
928 Centre, Berkeley, CA.
929
930 Ludwig, K.R. 2003. Isoplot: A Geochronological Toolkit for Microsoft Excel®.
931 Berkeley Geochronology Centre Special Publication No.4, 70pp., Berkeley
932 Geochronology Centre, Berkeley, CA. (Software version: Isoplot/Ex 3.41b, rev. 16
933 Nov 2005).
934
935 Mao, J.R., Li, Z.L., & Ye, H.M. 2014. Mesozoic tectono-magmatic activities in South
936 China: Retrospect and prospect. *Science China: Earth Sciences,* **57,** 2853–2877.
937
938 McPhie, J., Doyle, M. & Allen, R. 1993. *Volcanic Textures: A guide to the*
939 *interpretation of textures in volcanic rocks*. Tasmania Government Printing Office,
940 Tasmania.
941
942 Nemchin, A.A. & Cawood, P.A. 2005, Discordance of the U–Pb system in detrital
943 zircons: Implication for provenance studies of sedimentary rocks. *Sedimentary*
944 *Geology,* **182,** 143–162.
945
946 Pearce N.J.G., Perkins W.T., Westgate J.A., Gorton M.P., Jackson S.E., Neal C.R. &
947 Chenery S.P. 1997. A compilation of new and published major and trace element data
948 for NIST SRM 610 and NIST SRM 612 glass reference materials. *Geostandards*
949 *Newsletter,* **21,** 115–144.
950

951 Rubatto, D. 2002. Zircon trace element geochemistry: partitioning with garnet and the
952 link between U–Pb ages and metamorphism. *Chemical Geology,* **249,** 123–138.
953
954 Scherer, E., Munker, C., & Mezger, K. 2001. Calibration of the Lutetium–Hafnium
955 clock: *Science* **293,** 683–687.
956
957 Sewell, R.J., & Campbell, S.D.G. 1997. Geochemistry of coeval Mesozoic plutonic
958 and volcanic suites of Hong Kong. *Journal of the Geological Society, London,* **154,**
959 1053–1066.
960
961 Sewell, R.J., Campbell, S.D.G., Fletcher, C.J.N., Lai, K.W. & Kirk, P.A. 2000. *The*
962 *Pre-Quaternary Geology of Hong Kong*, Geotechnical Engineering Office. The
963 Government of the Hong Kong Special Administrative Region.
964
965 Sewell, R.J., Darbyshire, D.P.F., Langford, R.L. & Strange, P. J. 1992. Geochemistry
966 and Rb–Sr geochronology of Mesozoic granites from Hong Kong. *Transactions of the*
967 *Royal Society of Edinburgh (Earth Sciences),* **83,** 269–280.
968
969 Sewell, R.J., Davis, D.W. & Campbell, S.D.G. 2012. High precision U–Pb zircon ages
970 for Mesozoic igneous rocks from Hong Kong, *Journal of Asian Earth Sciences,* **43,**
971 164–175, doi:10.1016/j.jseaes.2011.09.007.
972
973 Sewell, R.J., Carter, A. & Rittner, M. 2016. Middle Jurassic collision of an exotic
974 microcontinental fragment: Implications for magmatism across the Southeast China
975 continental margin. *Gondwana Research,* **38,** 304–312.
976
977 Shi, H. & Li, C.F. 2012. Mesozoic and early Cenozoic tectonic convergence-to-rifting
978 transition prior to opening of the South China Sea. *International Geology Review,* **54,**
979 1801–1828.
980
981 Shu, L.S., Zhou, X.M., Deng, P., Wang, B., Jiang, S.Y., Yu, J.H. & Zhao, X.X. 2009.
982 Mesozoic tectonic evolution of the southeast china block: new insights from basin
983 analysis. *Journal of Asian Earth Sciences,* **34,** 376–391.
984
985 Sláma, J., Košler, J., Condon, D.J., Crowley, J.L., Gerdes, J.M., Hanchar, A.,
986 Horstwood, M.S.A., Morris, G.A., Nasdala, L., Norberg, N., Schaltegger, U., Schoene,
987 B., Tubrett, M.N. & Whitehouse, M.J. 2008. Plešovice zircon - A new natural
988 reference material for U–Pb and Hf isotopic microanalysis. *Chemical Geology,* **249,**

1–35.

So, K.W.F. & Sewell, R.J. 2017. *Guidelines on the description and classification of rocks of the Tuen Mun Formation in the Tuen Mun valley, Northwestern New Territories*. GEO Report No. 327. Geotechnical Engineering Office, Civil Engineering and Development Department, Hong Kong SAR Government. http://www.cedd.gov.hk/eng/publications/geo/rocks_tm.html

Song, S.R. & Lo, H.J. 2002. Lithofacies of volcanic rocks in the central Coastal Range, eastern Taiwan: implications for island arc evolution. *Journal of Asian Earth Sciences,* **21,** 23–38.

Tang, L.K. 2007. *Geology of Tuen Mun Area, NW Hong Kong: an updated Model*. M. Phil Thesis, University of Hong Kong.

Urban Planning Land and Resources Commission of Shenzhen Municipality (UPLRCSM) 2007. 1:50,000-scale Geological Map of Shenzhen. Report on Survey of the Shenzhen Geological Environment. (In Chinese)

Vermeesch, P. 2012. On the visualization of detrital age distributions: *Chemical Geology,* **312–313,** 190–194.

Vermeesch, P. 2013. Multisample comparison of detrital age distributions. *Chemical Geology,* **341,** 140–146.

Wang, D. & Shu, L. 2012. Late Mesozoic basin and range tectonics and related magmatism in Southeast China. *Geoscience Frontiers,* **3,** 109–124.

Wang, J.Q., Shu, L.S., Santosh, M. & Xu, Z.Q. 2015. The Pre-Mesozoic crustal evolution of the Cathaysia Block, South China: Insights from geological investigation, zircon U–Pb geochronology, Hf isotope and REE geochemistry from the Wugongshan complex. *Gondwana Research,* **28,** 225–245.

Watson, E.B. & Harrison, T.M. 1983. Zircon saturation revisted: temperature and composition effects in a variety of crustal magma types. *Earth and Planetary Science Letters,* **64,** 295–304.

White, J.D.L. & Busby-Spera, C.J. 1987. Deep marine arc apron deposits and syndepositional magmatism in the Alisitos group at Punta Cono, Baja California, Mexico. *Sedimentology,* **34,** 911–927.

White, J.D.L., McPhie, J. & Skilling, I. 2000. Peperite: a useful genetic term. *Bulletin of Volcanology,* **62,** 65–66.

White, M.J. & McPhie, J. 1996. Stratigraphy and palaeovolcanology of the Cambrian Tyndall Group, Mt Read Volcanics, western Tasmania. *Australian Journal of Earth Sciences,* **43,** 147–159.

White, M.J. & McPhie, J. 1997. A submarine welded ignimbrite-crystal rich sandstone facies association in the Cambrian Tyndall Group, western Tasmania. *Journal of Volcanology and Geothermal Research,* **76,** 277–295.

Wood, J. & Wallace, H. 1986. Volcanology and Mineral Deposits, Ontario Geological Survey, Miscellaneous Paper, **129,** 26.

Woodhead, J.D. & Hergt, J.M. 2005. A preliminary appraisal of seven natural zircon reference materials for in situ Hf isotope determination. *Geostandards and Geoanalytical Research,* **29,** 183–195.

Yao, J., Shu, L. & Santosh, M. 2011. Detrital zircon U–Pb geochronology, Hf-isotopes and geochemistry: New clues for the Precambrian crustal evolution of Cathaysia Block, South China. *Gondwana Research,* **20,** 553–567.

Yao, W.H., Li, Z.X., Li, W.X., Li, X.H. & Yang, J.H. 2014. From Rodinia to Gondwanaland: A tale of detrital zircon provenance analyses from the southern Nanhua Basin, South China. *American Journal of Science,* **314,** 278–313.

Zharikov, V., Pertsev, N., Rusinov, V., Callegari, E. & Fettes, D. 2007. Metasomatism and Metasomatic Rocks. *In:* Fettes, D. & Desmons, J. (eds) *Metamorphic Rocks: A Classification and Glossary of Terms.* Recommendations of the International Union of Geological Sciences (IUGS), Subcommission of the Systematics of Metamorphic Rocks, Cambridge University Press, Cambridge, 58–68.

Zhen, Y.M. (compiler) 1988. *Geological map of Shenzhen of the People's Republic of China 1:50000 (with explanatory text)*. Geological Publishing House, Beijing.

Zhou, X., Sun, T., Shen, W., Shu, L. & Niu, Y. 2006. Petrogenesis of Mesozoic granitoids and volcanic rocks in South China: a response to tectonic evolution. *Episodes,* **29,** 26–33.

Figure Captions:

Fig. 1. Location map of study area showing sample locations for detrital zircon geochronology and representative stratigraphic drillholes.

Fig. 2. Representative stratigraphic drillhole logs for the Tuen Mun Formation. Drllhole locations are shown on Figure 1. Slst = Siltstone, Sst = Sandstone, Congl = Conglomerate. Jut = Tin Shui Wai Member, Jus = Siu Hang Tsuen Member, Jua = Tuen Mun Andesite Member.

Fig. 3. Kernel density plots (Vermeesch 2012) of detrital zircon U–Pb ages of analysed samples compared with detrital zircon U–Pb ages of late Palaeozoic and Early to Middle Jurassic sedimentary rocks from adjacent areas (Data from Sewell *et al.* 2016).

Fig. 4. CL images of representative zircons from the youngest age fraction in six of the analysed samples.

Fig. 5. $\varepsilon_{Hf}(t)$ vs. U–Pb zircon age for the Tuen Mun Formation (HK13457) and late Palaeozoic and Early to Middle Jurassic rocks from adjacent areas. Comparison data from Sewell *et al.* (2016). CHUR = Chondritic Uniform Reservoir; DM = depleted mantle.

Fig. 6. (**a**) Thinly laminated crystal-rich tuffaceous sandstone interbedded with polymictic marble clast-bearing tuffaceous conglomerate exposed at Ling Tao Monastery, Ha Tsuen. Note load structures in sandstone at basal contact with polymictic conglomerate; (**b**) Polymictic, marble clast-bearing tuffaceous conglomerate and sandstone showing evidence of cross-bedding; (**c**) Andesite sill intruding polymictic tuffaceous conglomerate at Ling Tao Monastery showing evidence of magma-sediment mingling; (**d**) Polymictic, tuffaceous conglomerate exposed at Por Lo Shan, lower Tuen Mun valley. Clasts consist of andesite, coarse ash tuff and quartz sandstone; (**e**) Massive lava flows exposed in the western foothills of

the lower Tuen Mun valley; (**f**) Andesitic autobreccia exposed in the lower Tuen Mun valley.

Fig. 7. (**a**) Mylonitic tuffaceous breccia with many marble clasts, intruded by andesite in drillhole TMA50, Tuen Mun Area 52; (**b**) Calcareous metasandstone with occasional marble and quartzite clasts in drillhole BGS18, central Tuen Mun valley; (**c**) Mylonitic marble breccia in drillhole TSW27, northern Tuen Mun valley; inset is an example of skeletal residuum; (**d**) Altered tuffaceous sandstone with many quartzite clasts, and andesite showing evidence of mingling and reaction producing hydrothermal alteration in drillhole TMA59, eastern Tuen Mun valley; (**e**) Altered polymictic tuffaceous conglomerate with many marble clasts, and andesite intrusions. Garnet and epidote indicate intensive metasomatism and hydrothermal alteration (see inset). Drillhole TM22, central Tuen Mun valley; (**f**) Altered, calcareous, polymicitic tuffaceous breccia showing evidence of cyclical grading in drillhole BH3, Siu Hang Tsuen; (**g**) Andesite. Autobrecciated andesite lava flow in drillhole BH10, lower Tuen Mun valley; (**h**) Altered andesite hyaloclastite in drillhole NDH48, central Tuen Mun valley, showing evidence of reaction on margins of angular, lapilli- to block-sized lithic fragments. Scale Bar: 50 mm.

Fig. 8. (**a**) Photomicrograph showing boundary between marble clast and tuffaceous matrix, HK7797, Ha Tsuen; (**b**) Photomicrograph showing clast of quartzphyric rhyolite in tuffaceous matrix, HK7796, Ha Tsuen; (**c**) Photomicrograph of andesite clasts in polymictic, tuffaceous conglomerate, HK2732, Yuen Tau Shan; (**d**) Photomicrograph of quartz sandstone clast in polymictic conglomerate, BGS15, HK7781, Ha Tsuen; (**e**) Porphyritic andesite, HK9663, San Shek Wan; (**f**) Andesitic, crystal-rich ash tuff, HK10247, Leung King Estate. Scale Bar: 0.5 mm.

Fig. 9. Cumulative proportion curves of zircon age data (after Cawood *et al.* 2012) for the Tuen Mun Formation showing the relationship between crystallization age, depositonal age and tectonic setting. A = convergent margin; B = collisional; C = extensional.

Fig. 10. Multidimensional scaling (MDS) map that compares detrital zircon U–Pb age distributions for each of the analysed samples with samples from adjacent Carboniferous and E. to Mid. Jurassic rocks (Data from Sewell *et al.* 2016). The MDS map provides a visualization of Kolmogorov-Smirnov distances between samples and shows which samples are similar to each other (cluster) and which are different

(spaced apart). The solid lines mark the closest neighbours and dashed lines the second closest neighbour. Values on the X and Y axes represent a normalised distance.

Fig. 11. Depositional model for the Tuen Mun Formation (based on Wood & Wallace 1986).

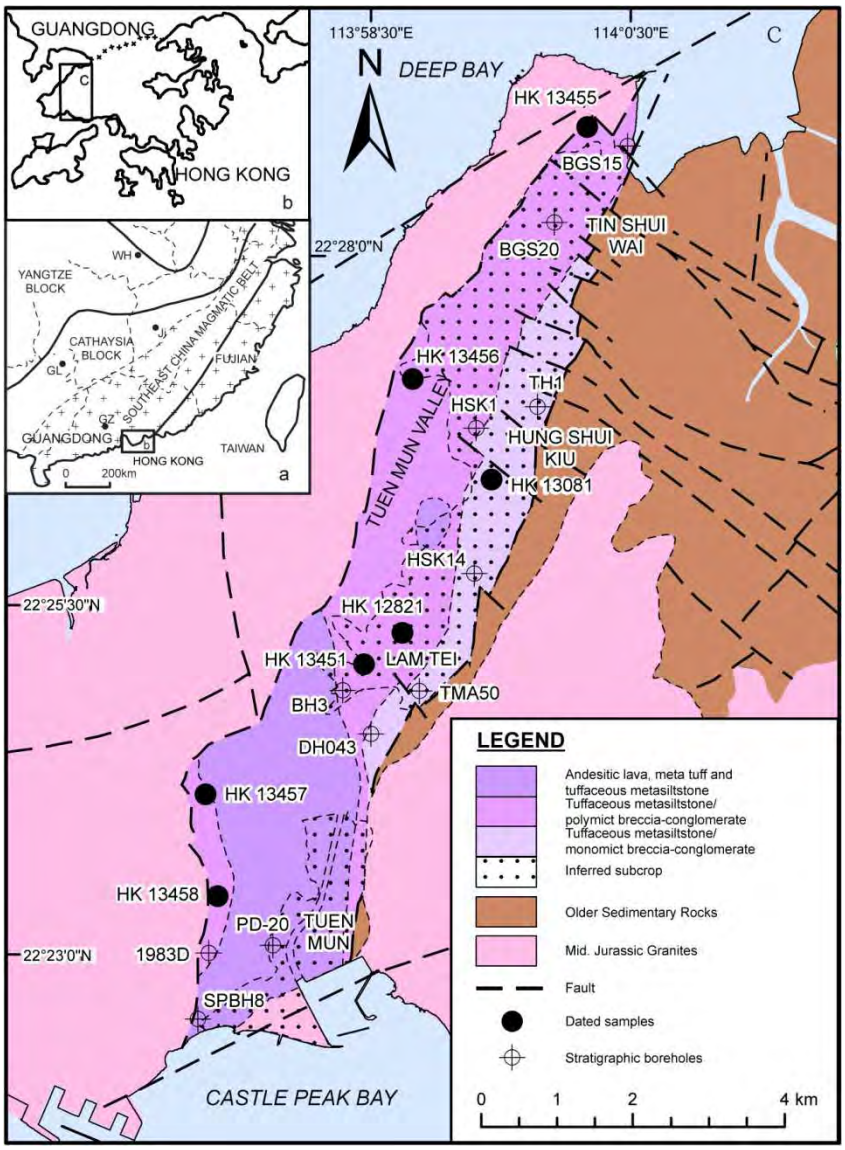
GUANGDONG
HONG KONG
b
c
WH
YANGTZE BLOCK
CATHAYSIA BLOCK
GL
GZ
SOUTHEAST CHINA MAGMATIC BELT
FUJIAN
GUANGDONG
HONG KONG
TAIWAN
0 200km
a
113°58'30"E
114°0'30"E
C
N
DEEP BAY
22°28'0"N
22°25'30"N
22°23'0"N
HK 13455
BGS15
TIN SHUI WAI
BGS20
HK 13456
TH1
HSK1
HUNG SHUI KIU
HK 13081
TUEN MUN VALLEY
HSK14
HK 12821
HK 13451
LAM TEI
TMA50
BH3
DH043
HK 13457
HK 13458
PD-20
TUEN MUN
1983D
SPBH8
CASTLE PEAK BAY
LEGEND
Andesitic lava, meta tuff and tuffaceous metasiltstone
Tuffaceous metasiltstone/ polymict breccia-conglomerate
Tuffaceous metasiltstone/ monomict breccia-conglomerate
Inferred subcrop
Older Sedimentary Rocks
Mid. Jurassic Granites
Fault
Dated samples
Stratigraphic boreholes
0 1 2 4 km

Figure 1

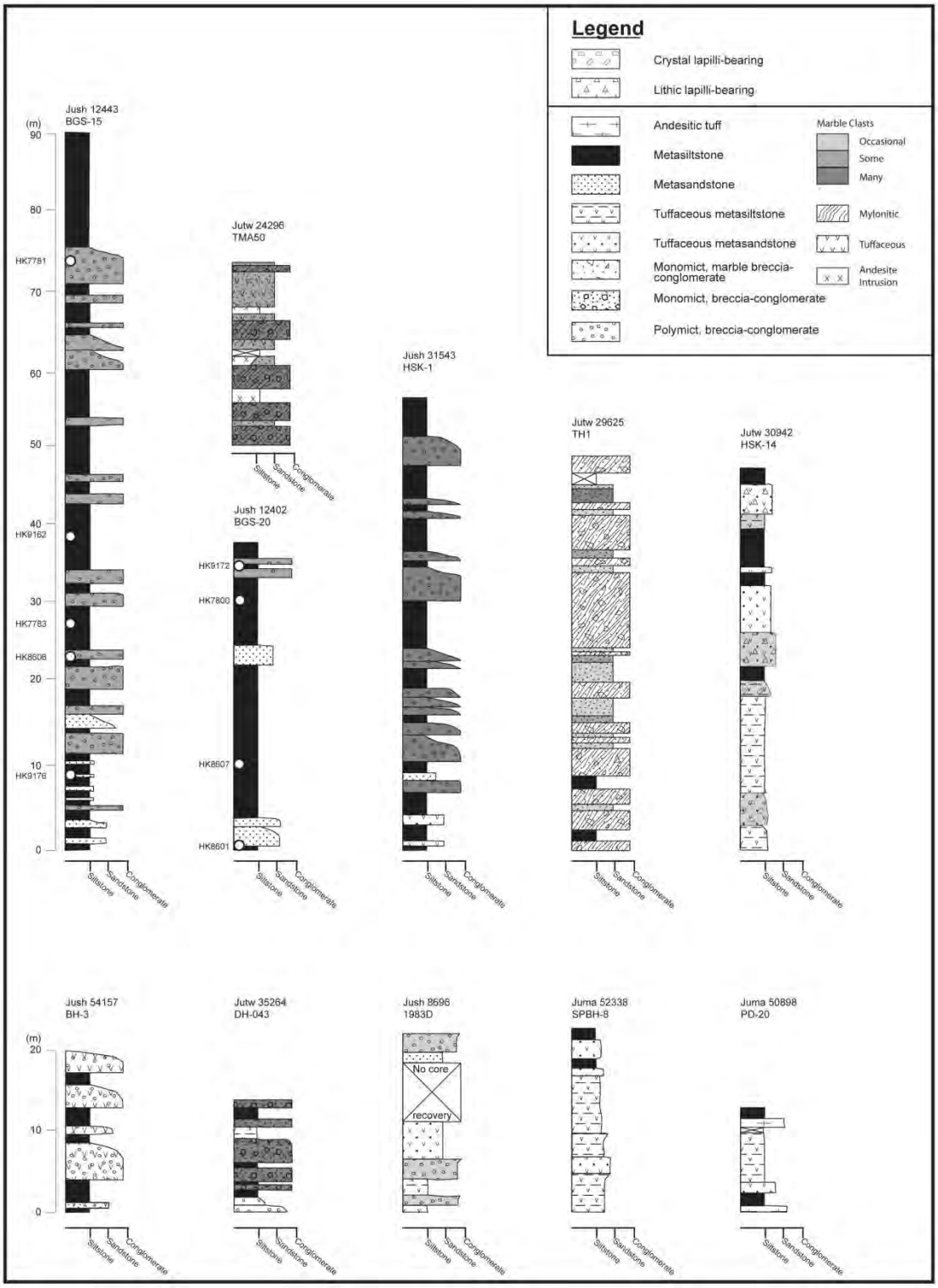
Legend
Crystal lapilli-bearing
Lithic lapilli-bearing
Andesitic tuff
Metasiltstone
Metasandstone
Tuffaceous metasiltstone
Tuffaceous metasandstone
Monomict, marble breccia-conglomerate
Monomict, breccia-conglomerate
Polymict, breccia-conglomerate
Marble Clasts
Occasional
Some
Many
Mylonitic
Tuffaceous
Andesite Intrusion
Jush 12443
BGS-15
Jutw 24296
TMA50
Jush 12402
BGS-20
Jush 31543
HSK-1
Jutw 29625
TH1
Jutw 30942
HSK-14
Jush 54157
BH-3
Jutw 35264
DH-043
Jush 8696
1983D
No core recovery
Juma 52338
SPBH-8
Juma 50898
PD-20
Siltstone
Sandstone
Conglomerate
(m)

Figure 2

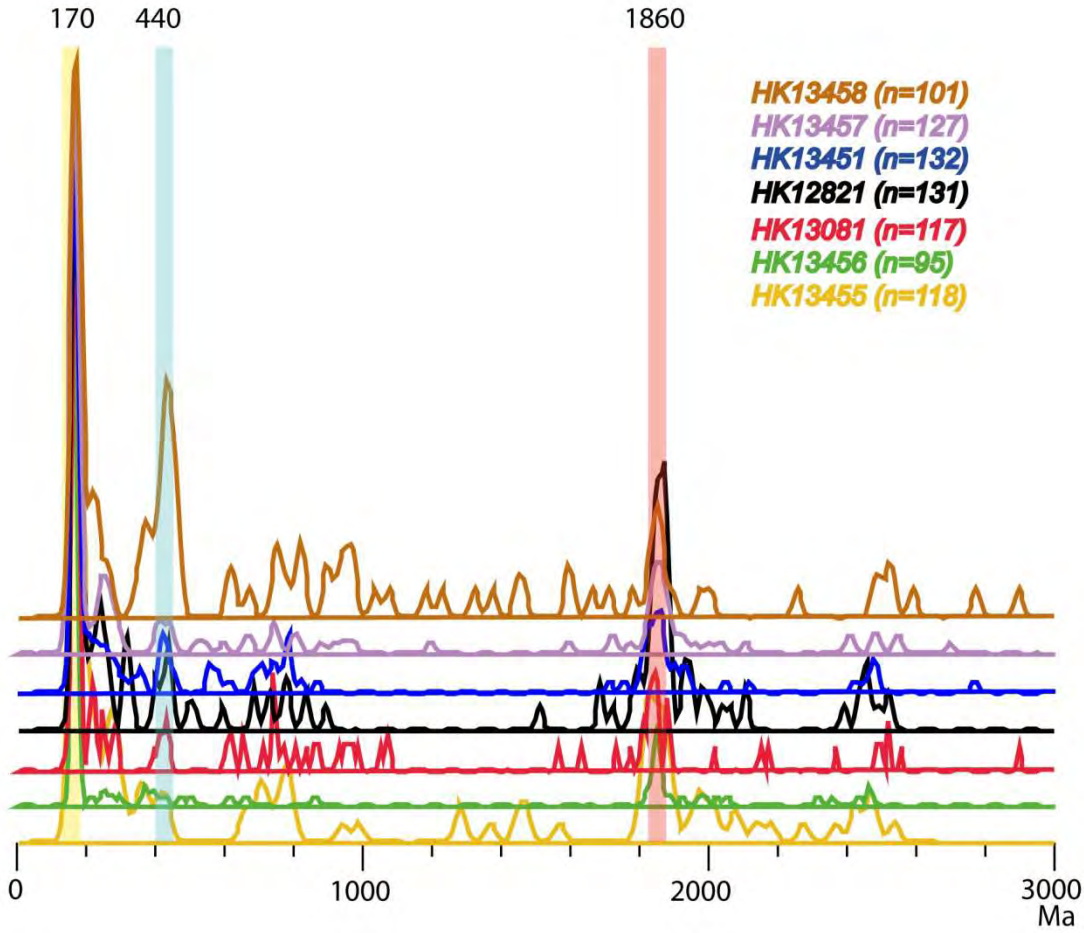
170
440
1860
HK13458 (n=101)
HK13457 (n=127)
HK13451 (n=132)
HK12821 (n=131)
HK13081 (n=117)
HK13456 (n=95)
HK13455 (n=118)
0
1000
2000
3000
Ma

Figure 3


HK13455
G26-168Ma
G58-174Ma
G70-169Ma
G84-169Ma
G89-179Ma
G103-172Ma
50μm
HK13456
G4-162Ma
G19-168Ma
G69-172Ma
G101-166Ma
G114-178Ma
G145-173Ma
50μm
HK13457
G1-170Ma
G6-171Ma
G50-170Ma
G75-174Ma
G81-171Ma
G112-170Ma
50μm
HK13458
G14-171Ma
G25-164Ma
G36-172Ma
G40-176Ma
G46-161Ma
G70-170Ma
50μm
HK13451
G52-168Ma
G9-163Ma
G52-168Ma
G73-166Ma
G97-174Ma
G112-174Ma
50μm
HK12821
G53-168Ma
G61-171Ma
G66-175Ma
G112-171Ma
G139-163Ma
G149-176Ma
50μm
Figure 4

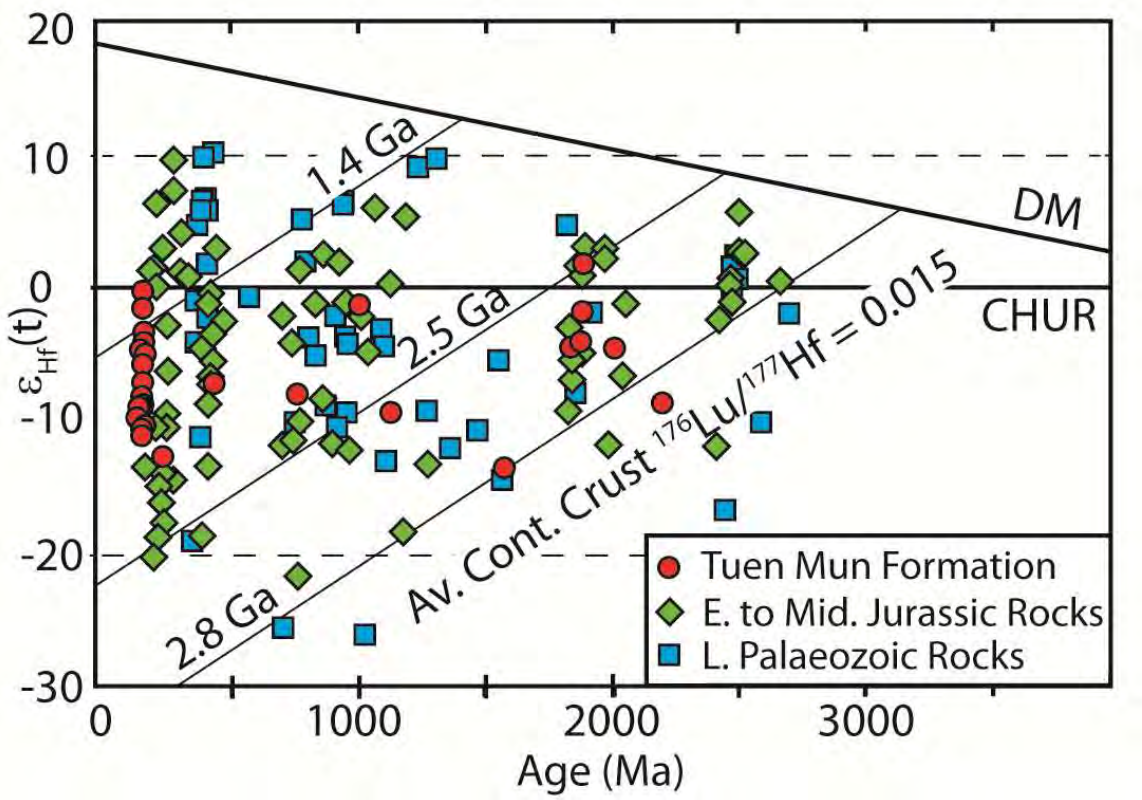
20
10
0
-10
-20
-30
$\varepsilon_{Hf}(t)$
0
1000
2000
3000
Age (Ma)
1.4 Ga
2.5 Ga
2.8 Ga
DM
CHUR
Av. Cont. Crust $^{176}Lu/^{177}Hf = 0.015$
Tuen Mun Formation
E. to Mid. Jurassic Rocks
L. Palaeozoic Rocks

Figure 5

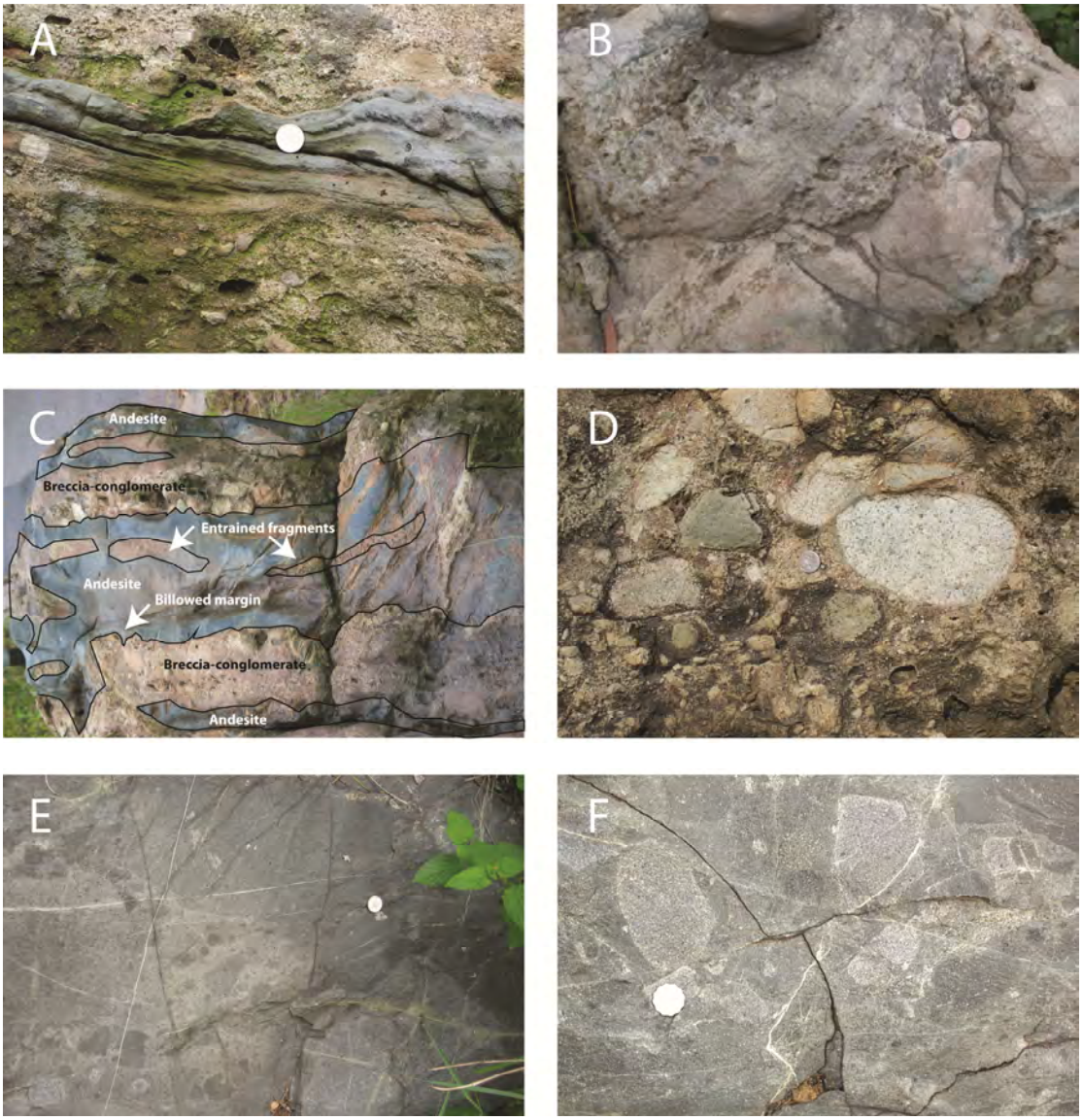
A
B
C
Andesite
Breccia-conglomerate
Entrained fragments
Andesite
Billowed margin
Breccia-conglomerate
Andesite
D
E
F

Figure 6

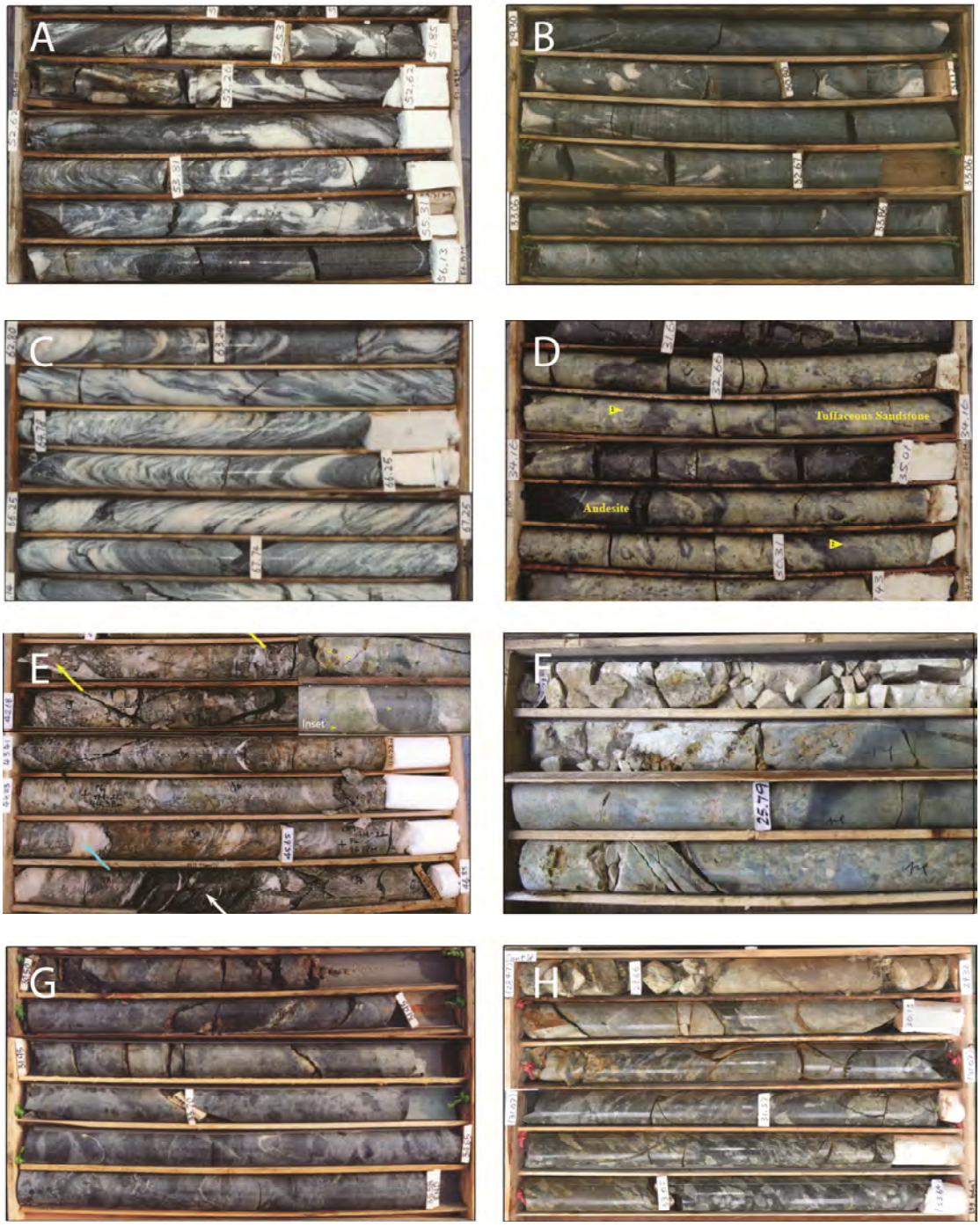

Figure 7

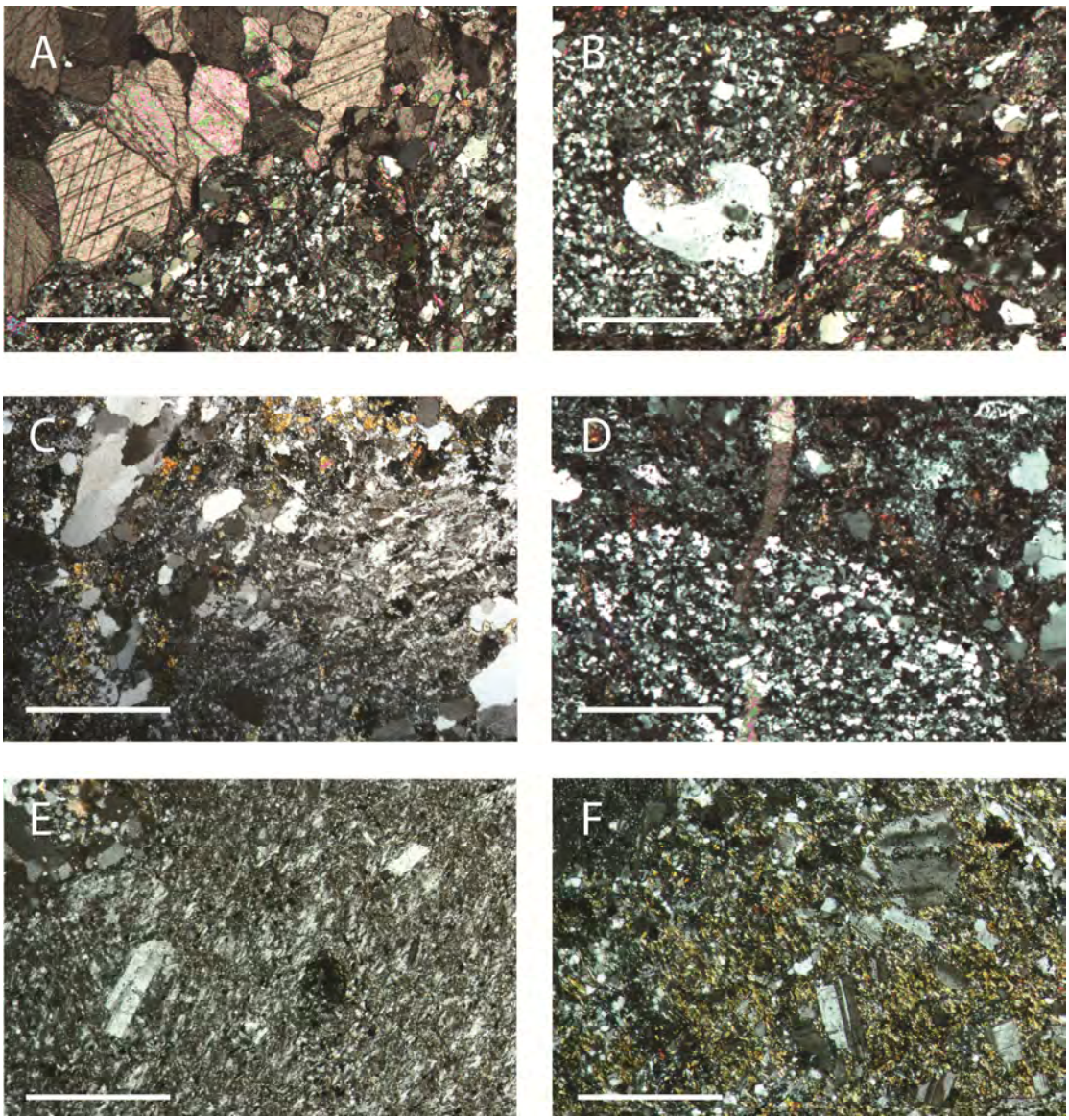

Figure 8

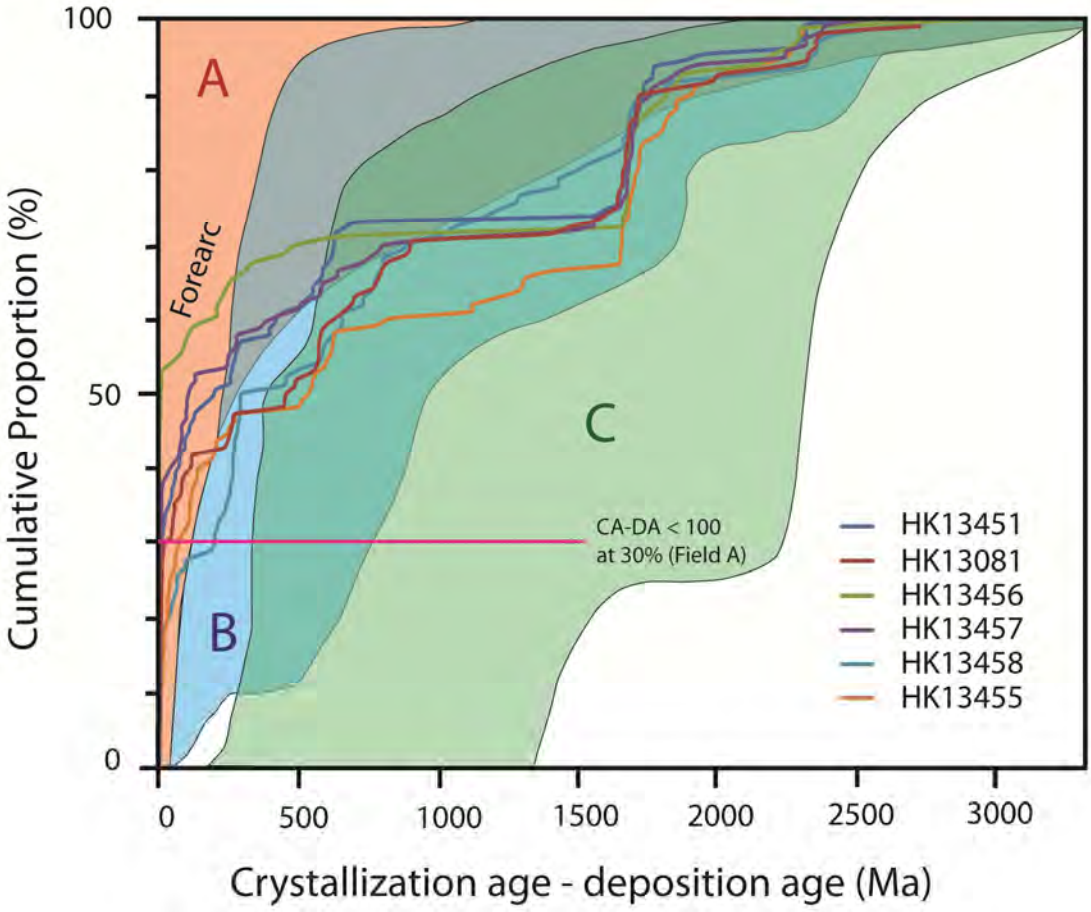
100
50
0
A
Forearc
B
C
CA-DA < 100
at 30% (Field A)
HK13451
HK13081
HK13456
HK13457
HK13458
HK13455
Cumulative Proportion (%)
0
500
1000
1500
2000
2500
3000
Crystallization age - deposition age (Ma)

Figure 9

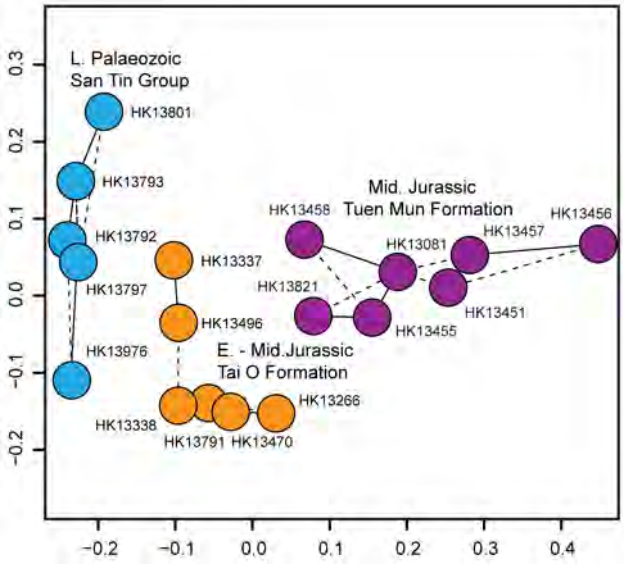
L. Palaeozoic
San Tin Group
HK13801
HK13793
HK13792
HK13797
HK13976
HK13337
HK13496
E. - Mid.Jurassic
Tai O Formation
HK13338
HK13791
HK13470
HK13266
Mid. Jurassic
Tuen Mun Formation
HK13458
HK13821
HK13455
HK13081
HK13457
HK13451
HK13456
0.3
0.2
0.1
0.0
−0.1
−0.2
−0.2
−0.1
0.0
0.1
0.2
0.3
0.4

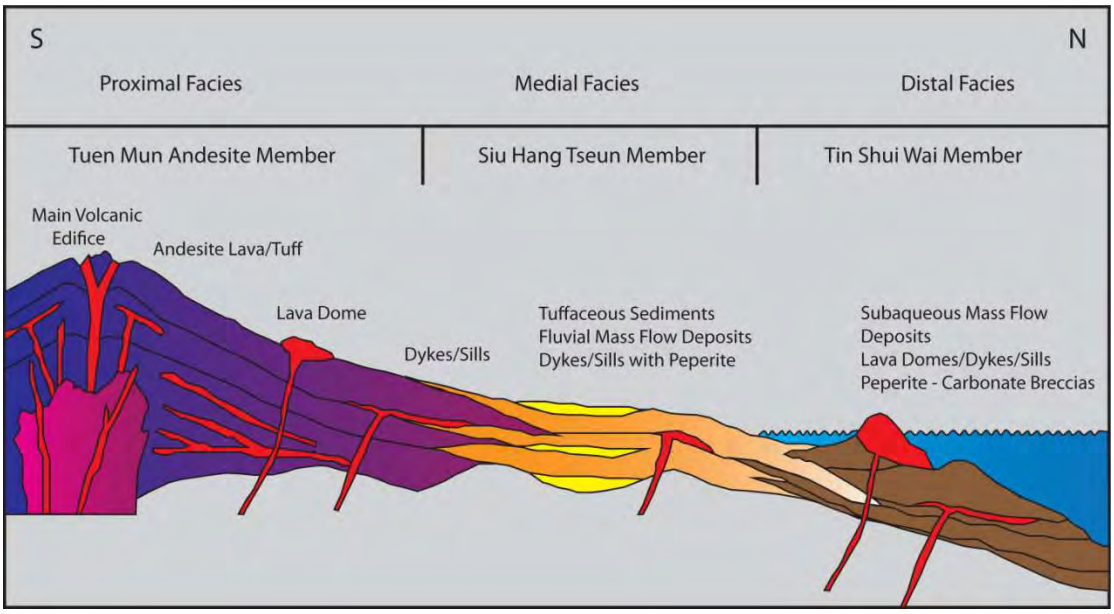
S
N
Proximal Facies
Medial Facies
Distal Facies
Tuen Mun Andesite Member
Siu Hang Tseun Member
Tin Shui Wai Member
Main Volcanic Edifice
Andesite Lava/Tuff
Lava Dome
Dykes/Sills
Tuffaceous Sediments
Fluvial Mass Flow Deposits
Dykes/Sills with Peperite
Subaqueous Mass Flow Deposits
Lava Domes/Dykes/Sills
Peperite - Carbonate Breccias

Figure 11

Table 1
History of nomenclature for rocks of the Tuen Mun Formation

Langford et al. 1989	Frost 1992	Sewell et al. 2000	This Paper	
Tuen Mun Formation	Tuen Mun Formation	Tuen Mun Formation	Tuen Mun Fm	Tuen Mun Andesite Member
				Sui Hang Tsuen Member
Tsing Shan Formation	Tin Shui Wai Member			Tin Shui Wai Member

Table 2
U–Pb data on zircon from sedimentary rocks in the Tuen Mun Valley area, Hong Kong.

Grain	Measured Ratios						Pb	U	Th/U	Corrected Ages (Ma)						
	$^{206}Pb\dagger/^{238}U$	1σ	$^{207}Pb\dagger/^{235}U$	1σ	$^{207}Pb\dagger/^{206}Pb$	1σ	(ppm)	(ppm)	Atomic	$^{206}Pb\dagger/^{238}U$	2σ	$^{207}Pb\dagger/^{235}U$	2σ	$^{207}Pb\dagger/^{206}Pb$	2σ	% Disc.
Sample 13455																
G1	0.0261	0.0003	0.1789	0.0079	0.0500	0.0009	28.1	629.5	2.51	165.9	4.9	167.1	7.3	193.1	6.7	0.7
G3	0.3378	0.0040	5.6735	0.2354	0.1213	0.0008	113.2	319.2	0.32	1876.3	38.9	1927.3	24.2	1976.0	12.8	5.0
G5	0.0252	0.0003	0.1788	0.0079	0.0496	0.0008	7.9	283.0	0.64	160.2	4.6	167.0	6.9	178.2	6.1	4.1
G6	0.0433	0.0005	0.3144	0.0135	0.0528	0.0007	27.7	604.9	0.48	273.1	7.3	277.6	9.6	319.8	8.2	1.6
G8	0.1071	0.0013	1.0057	0.0431	0.0629	0.0008	32.9	255.6	0.87	655.9	16.0	706.7	17.7	704.5	13.3	7.2
G9	0.1301	0.0016	1.3041	0.0556	0.0674	0.0008	38.0	233.8	1.04	788.2	18.8	847.5	19.4	849.2	14.0	7.0
G10	0.2554	0.0030	3.6559	0.1527	0.0971	0.0008	88.8	244.0	1.57	1466.0	31.8	1561.8	23.0	1569.5	13.2	6.6
G11	0.3792	0.0045	8.0790	0.3374	0.1439	0.0011	102.7	242.7	0.52	2072.4	42.8	2239.9	25.7	2274.2	14.0	8.9
G13	0.0259	0.0003	0.1864	0.0083	0.0509	0.0009	9.5	328.1	0.67	164.7	4.9	173.6	7.6	234.9	8.2	5.1
G14	0.0574	0.0007	0.4298	0.0181	0.0538	0.0005	36.7	561.9	0.70	360.0	9.1	363.0	10.2	364.4	6.8	0.8
G15	0.0263	0.0003	0.1828	0.0078	0.0498	0.0006	17.7	639.1	0.46	167.5	4.7	170.4	6.0	183.3	4.8	1.7
G16	0.3147	0.0037	4.8162	0.2004	0.1113	0.0008	189.6	608.3	0.12	1763.9	37.1	1787.7	23.8	1820.4	12.6	3.1
G17	0.0268	0.0003	0.2065	0.0089	0.0555	0.0008	13.6	460.0	0.62	170.2	4.9	190.6	7.0	432.4	10.2	10.7
G18	0.3337	0.0040	5.9526	0.2490	0.1279	0.0010	168.5	460.7	0.47	1856.0	39.1	1968.9	25.2	2069.6	14.1	10.3
G21	0.0470	0.0006	0.3583	0.0151	0.0544	0.0005	45.7	907.1	0.49	296.3	7.6	310.9	8.8	386.8	6.9	4.7
G23	0.0258	0.0003	0.1779	0.0078	0.0494	0.0008	12.4	369.1	1.23	164.1	4.7	166.2	6.7	167.8	5.4	1.2
G24	0.0664	0.0008	0.5366	0.0230	0.0584	0.0007	31.2	382.8	0.99	414.2	10.6	436.2	13.1	544.8	11.2	5.0
G25	0.3463	0.0041	5.7315	0.2395	0.1192	0.0009	161.3	461.4	0.14	1917.0	40.1	1936.1	24.8	1944.0	13.5	1.4
G26	0.0264	0.0003	0.1808	0.0078	0.0494	0.0006	15.8	565.3	0.49	167.9	4.7	168.8	6.2	165.4	4.7	0.5
G27	0.0434	0.0006	0.3290	0.0147	0.0526	0.0010	14.2	327.4	0.25	273.7	7.6	288.8	11.5	310.7	10.4	5.2
G28	0.4213	0.0050	#####	0.4219	0.1607	0.0013	135.7	258.4	0.97	2266.2	46.4	2439.8	26.9	2463.5	15.1	8.0
G29	0.0409	0.0005	0.2949	0.0126	0.0518	0.0006	22.7	498.3	0.64	258.5	6.9	262.4	8.6	275.7	6.5	1.5
G30	0.2998	0.0037	5.1004	0.2183	0.1163	0.0012	56.4	181.8	0.26	1690.5	37.4	1836.2	27.5	1900.1	18.0	11.0
G32	0.0259	0.0004	0.2019	0.0098	0.0530	0.0014	6.9	244.7	0.58	164.9	5.4	186.7	10.5	327.9	15.6	11.7
G36	0.0260	0.0003	0.1846	0.0080	0.0510	0.0007	17.9	617.2	0.65	165.5	4.7	172.0	6.4	240.4	6.4	3.8
G37	0.3284	0.0040	5.1750	0.2184	0.1142	0.0010	126.4	375.9	0.22	1830.6	39.1	1848.5	25.9	1866.8	15.4	1.9
G39	0.1313	0.0016	1.2863	0.0548	0.0671	0.0007	45.0	270.0	1.11	795.3	18.9	839.7	18.6	840.3	12.6	5.3
G40	0.1284	0.0016	1.1899	0.0504	0.0672	0.0006	75.7	547.5	0.48	778.7	18.5	795.9	17.7	844.6	11.6	2.2
G41	0.0486	0.0006	0.3943	0.0172	0.0582	0.0009	16.4	307.6	0.61	305.7	8.2	337.5	11.7	538.8	12.9	9.4
G43	0.0382	0.0006	0.2960	0.0148	0.0516	0.0015	5.1	126.5	0.44	241.9	7.7	263.3	14.7	267.7	14.2	8.1
G44	0.3273	0.0040	5.0554	0.2141	0.1117	0.0010	172.7	429.3	0.90	1825.3	39.2	1828.7	26.3	1827.7	16.0	0.1
G46	0.0262	0.0004	0.1976	0.0101	0.0507	0.0016	5.7	190.0	0.74	166.4	5.6	183.1	11.5	226.3	13.4	9.1
G47	0.3461	0.0042	5.9460	0.2520	0.1241	0.0011	413.3	1199.6	0.11	1916.0	40.8	1968.0	27.1	2015.9	16.8	5.0
G48	0.1170	0.0015	1.1204	0.0494	0.0654	0.0010	33.7	239.9	0.91	713.3	18.0	763.2	21.1	787.6	17.0	6.5
G49	0.2992	0.0036	4.6777	0.1988	0.1128	0.0011	243.9	788.8	0.30	1687.5	36.8	1763.3	26.6	1845.2	17.0	8.5
G51	0.0257	0.0003	0.1887	0.0084	0.0533	0.0009	14.1	502.4	0.57	163.3	4.9	175.5	7.3	343.3	10.0	6.9
G52	0.4212	0.0052	9.5124	0.4057	0.1626	0.0016	404.1	932.3	0.19	2265.9	47.4	2388.7	29.7	2483.0	19.2	8.7
G53	0.1664	0.0021	1.6920	0.0727	0.0732	0.0008	74.0	399.2	0.62	992.0	23.4	1005.5	21.8	1018.4	14.9	2.6
G54	0.0349	0.0005	0.2656	0.0125	0.0541	0.0012	15.2	323.3	1.33	221.3	6.7	239.2	11.9	375.6	15.1	7.5
G55	0.2001	0.0025	2.3398	0.1004	0.0835	0.0009	89.7	420.4	0.45	1175.6	27.2	1224.5	24.0	1280.9	16.6	8.2
G56	0.4145	0.0051	9.3276	0.4007	0.1570	0.0017	100.8	219.4	0.48	2235.6	47.4	2370.7	30.6	2423.6	20.4	7.8
G57	0.0263	0.0004	0.1811	0.0084	0.0494	0.0011	10.7	349.3	0.83	167.5	5.2	169.0	8.6	165.0	7.2	0.8
G58	0.0274	0.0004	0.1879	0.0082	0.0497	0.0007	28.2	909.1	0.70	174.0	5.1	174.9	6.9	179.1	5.4	0.5
G60	0.3112	0.0039	4.7613	0.2050	0.1109	0.0012	304.0	946.7	0.26	1746.5	38.6	1778.1	28.7	1814.9	19.6	3.8
G62	0.1191	0.0015	1.1683	0.0512	0.0711	0.0010	51.5	407.4	0.50	725.2	18.1	785.8	21.2	961.4	17.8	7.7
G63	0.0275	0.0004	0.2011	0.0099	0.0501	0.0013	8.8	280.9	0.71	174.8	5.7	186.0	10.6	197.3	10.3	6.0
G64	0.4184	0.0053	9.2847	0.4051	0.1523	0.0019	50.3	108.7	0.44	2253.2	48.7	2366.5	32.7	2371.8	23.1	5.0
G65	0.0276	0.0004	0.1891	0.0088	0.0500	0.0011	13.2	415.6	0.77	175.7	5.3	175.9	8.9	194.1	8.2	0.1
G66	0.0360	0.0005	0.2524	0.0112	0.0506	0.0008	19.5	429.9	1.08	228.2	6.4	228.5	8.9	223.6	6.9	0.1
G67	0.0591	0.0008	0.4531	0.0201	0.0538	0.0008	19.5	297.3	0.63	370.1	10.0	379.4	13.0	363.9	9.9	2.4
G68	0.1143	0.0015	1.1662	0.0533	0.0678	0.0012	#####	149.7	1.63	697.9	18.4	784.9	24.5	863.1	22.0	11.1
G69	0.1162	0.0015	1.1066	0.0500	0.0649	0.0011	13.2	82.0	1.48	708.6	18.4	756.5	23.1	769.5	19.2	6.3
G70	0.0266	0.0004	0.1824	0.0082	0.0495	0.0009	19.7	722.5	0.36	169.1	5.1	170.1	7.5	173.5	6.2	0.6
G71	0.3244	0.0041	5.3122	0.2323	0.1137	0.0015	103.6	296.0	0.41	1810.9	40.5	1870.8	31.4	1858.9	22.8	2.6
G73	0.4675	0.0059	#####	0.4547	0.1615	0.0021	231.0	447.7	0.36	2472.5	52.5	2471.3	34.2	2470.9	24.7	-0.1
G75	0.3535	0.0045	6.0039	0.2628	0.1223	0.0016	322.6	814.8	0.52	1951.1	43.2	1976.4	32.4	1990.0	23.7	2.0
G76	0.3448	0.0044	5.4602	0.2405	0.1127	0.0016	139.7	352.0	0.64	1909.5	42.8	1894.4	32.8	1843.2	24.1	-3.6
G77	0.0258	0.0003	0.1803	0.0082	0.0505	0.0009	14.1	451.1	0.95	164.0	5.0	168.3	7.7	218.5	7.9	2.5
G78	0.0264	0.0004	0.1798	0.0083	0.0494	0.0010	13.4	463.4	0.59	167.7	5.1	167.9	8.2	165.9	6.9	0.2
G80	0.3226	0.0042	5.2577	0.2339	0.1113	0.0016	72.8	197.5	0.62	1802.4	41.3	1862.0	33.7	1820.1	25.5	1.0
G81	0.0442	0.0006	0.3556	0.0168	0.0566	0.0013	16.7	334.2	0.69	278.9	8.2	308.9	14.3	475.6	17.5	9.7
G82	0.0427	0.0006	0.3603	0.0167	0.0584	0.0012	10.4	246.8	0.20	269.2	7.9	312.4	13.4	545.9	17.9	13.8
G83	0.3951	0.0051	8.9671	0.3992	0.1572	0.0023	108.4	239.2	0.65	2146.2	47.8	2334.7	36.4	2425.5	27.9	11.5
G84	0.0266	0.0004	0.1806	0.0083	0.0494	0.0009	15.3	567.3	0.33	168.9	5.1	168.5	7.9	165.4	6.5	-0.2
G85	0.0302	0.0004	0.2135	0.0100	0.0502	0.0011	10.1	301.4	0.65	191.6	5.8	196.5	9.6	202.4	8.6	2.5
G86	0.1576	0.0021	1.6392	0.0739	0.0717	0.0012	37.7	209.8	0.69	943.1	23.7	985.4	26.7	976.3	21.4	4.3
G88	0.0258	0.0004	0.1801	0.0089	0.0505	0.0014	10.6	364.3	0.71	164.0	5.4	168.2	10.1	216.7	11.1	2.5
G89	0.0282	0.0004	0.1922	0.0088	0.0495	0.0009	17.0	514.0	0.81	179.5	5.3	178.5	8.2	172.5	6.6	-0.5
G90	0.0266	0.0004	0.1852	0.0087	0.0495	0.0011	9.7	320.6	0.72	169.2	5.2	172.5	8.6	172.1	7.4	2.0
G91	0.3255	0.0043	5.3166	0.2400	0.1111	0.0018	63.7	192.1	0.19	1816.6	42.1	1871.5	36.1	1817.2	28.3	0.0
G92	0.0255	0.0004	0.1954	0.0097	0.0522	0.0014	7.4	243.3	0.89	162.4	5.4	181.2	10.5	292.9	14.7	10.4
G93	0.1261	0.0017	1.1448	0.0520	0.0658	0.0012	64.5	537.3	0.10	765.6	19.7	774.8	24.4	799.4	20.1	1.2
G94	0.0313	0.0004	0.2558	0.0121	0.0591	0.0013	14.0	363.6	1.09	198.7	6.2	231.3	11.6	571.9	20.2	14.1
G95	0.2136	0.0029	2.7115	0.1246	0.0874	0.0016	49.5	224.9	0.31	1248.2	31.2	1331.6	33.8	1368.2	28.1	8.8
G96	0.0304	0.0004	0.2214	0.0105	0.0518	0.0011	11.9	325.4	0.94	192.8	6.0	203.1	10.1	277.0	11.4	5.1
G98	0.3318	0.0044	5.2674	0.2395	0.1149	0.0020	142.0	417.0	0.22	1847.1	43.0	1863.6	37.8	1878.3	30.3	1.7
G99	0.1292	0.0017	1.2474	0.0573	0.0703	0.0013	59.3	385.5	0.82	783.2	20.5	822.2	26.5	938.0	23.3	4.7
G100	0.0305	0.0004	0.2233	0.0109	0.0535	0.0013	11.2	323.3	0.75	193.8	6.2	204.7	11.5	350.5	15.6	5.3
G101	0.2878	0.0038	4.3749	0.2010	0.1105	0.0020	197.5	695.2	0.13	1630.4	39.2	1707.6	38.3	1807.8	31.7	9.8
G102	0.0323	0.0005	0.2522	0.0120	0.0566	0.0013	16.2	454.6	0.62	204.8	6.3	228.3	11.4	474.8	17.5	10.3
G103	0.0271	0.0004	0.1844	0.0100	0.0499	0.0017	10.6	365.0	0.55	172.3	6.1	171.8	12.9	191.3	12.8	-0.3
G104	0.0344	0.0005	0.2543	0.0126	0.0506	0.0013	8.3	194.1	1.04	218.1	6.9	230.1	12.5	220.8	11.1	5.2
G105	0.2498	0.0034	3.2278	0.1502	0.0926	0.0018	57.1	199.6	0.69	1437.7	35.7	1463.9	37.5	1479.1	31.2	2.8
G106	0.3364	0.0046	6.5712	0.3073	0.1330	0.0026	63.9	166.1	0.64	1869.1	45.0	2055.5	42.7	2137.3	36.0	12.5
G107	0.0273	0.0004	0.2070	0.0105	0.0545	0.0016	8.3	274.8	0.64	173.4	5.9	191.0	11.9	393.0	19.4	9.3
G108	0.0549	0.0008	0.4722	0.0221	0.0627	0.0013	46.3	885.2	0.18	344.3	9.9	392.7	16.8	697.7	21.3	12.3
G109	0.3564	0.0049	6.0784	0.2842	0.1242	0.0025	144.5	345.9	0.73	1965.2	46.8	1987.2	43.0	2018.0	35.8	2.6
G110	0.0589	0.0008	0.4376	0.0206	0.0542	0.0011	60.7	878.3	0.81	369.0	10.6	368.5	16.2	379.0	13.9	-0.1
G111	0.4023	0.0049	9.5913	0.2842	0.1681	0.0025	108.1	247.4	0.41	2179.5	45.3	2396.3	35.7	2539.2	28.3	14.2
G112	0.1102	0.0008	1.0552	0.0206	0.0694	0.0011	78.6	740.3	0.19	673.7	10.1	731.4	19.3	910.7	20.3	7.9
G113	0.3403	0.0055	5.3277	0.4499	0.1141	0.0034	148.0	404.0	0.39	1888.3	53.5	1873.3	59.0	1865.1	51.9	-1.2
G114	0.0285	0.0015	0.1957	0.0498	0.0497	0.0015	12.7	416.3	0.51	181.2	19.8	181.5	21.0	182.9	10.6	0.2
G115	0.3499	0.0047	6.1926	0.2509	0.1291	0.0024	165.5	442.9	0.35	1934.1	45.3	2003.4	40.4	2085.5	33.2	7.3
G116	0.3305	0.0004	5.4980	0.0100	0.1151	0.0015	92.2	253.6	0.47	1840.7	4.9	1900.3	22.3	1882.1	22.3	2.2
G117	0.3388	0.0048	5.4106	0.2932	0.1154	0.0028	174.6	492.1	0.29	1880.7	47.2	1886.5	48.3	1885.5	41.6	0.3
G118	0.0477	0.0046	0.3858	0.2617	0.0588	0.0025	22.2	368.4	1.11	300.1	57.2	331.3	60.3	560.4	37.3	9.4
G119	0.2012	0.0047	2.3077	0.2572	0.0837	0.0025	76.8	319.9	0.86	1181.5	51.0	1214.6	54.5	1285.4	44.3	8.1
G121	0.0348	0.0028	0.2443	0.1108	0.0507	0.0019	29.1	644.6	1.20	220.8	35.8	221.9	36.1	225.8	15.8	0.5
G123	0.0298	0.0005	0.2353	0.0122	0.0557	0.0013	10.2	305.5	0.68	189.2	7.1	214.5	11.9	441.6	17.9	11.8
G125	0.0449	0.0005	0.3247	0.0120	0.0527	0.0016	43.1	834.6	0.75	283.3	6.3	285.5	16.5	315.0	17.0	0.8
G127	0.0368	0.0007	0.2578	0.0160	0.0510	0.0013	23.1	600.8	0.44	232.8	8.8	232.9	13.9	241.3	12.0	0.0
G129	0.3600	0.0005	6.0074	0.0129	0.1208	0.0014	144.0	382.1	0.27	1982.1	5.8	1976.9	20.8	1967.8	20.6	-0.7
G130	0.0281	0.0005	0.2041	0.0164	0.0501	0.0019	8.3	266.6	0.67	178.5	7.4	188.6	14.7	200.1	14.6	5.4
G133	0.0269	0.0043	0.2126	0.2798	0.0554	0.0034	8.6	292.6	0.59	171.0	55.1	195.7	60.3	430.0	43.5	12.6
G134	0.0306	0.0008	0.2195	0.0254	0.0521	0.0023	25.0	771.0	0.47	194.2	11.1	201.5	19.6	290.7	22.9	3.6
G135	0.0316	0.0004	0.2233	0.0111	0.0505	0.0017	10.9	325.4	0.48	200.6	5.8	204.7	13.9	217.6	13.8	2.0
G137	0.3817	0.0005	7.2181	0.0115	0.1365	0.0015	186.1	439.5	0.48	2084.2	5.2	2138.7	20.2	2182.9	20.2	4.5
G138	0.2211	0.0043	2.7630	0.2382	0.0910	0.0034	216.7	890.6	0.56	1287.8	45.6	1345.6	63.6	1446.4	58.5	11.0
G139	0.0267	0.0056	0.1958	0.3629	0.0498	0.0036	6.3	208.5	0.68	169.9	71.3	181.5	70.8	186.1	25.6	6.4
G140	0.3067	0.0033	4.8825	0.1389	0.1133	0.0025	110.9	346.6	0.32	1724.4	32.8	1799.2	41.2	1852.5	37.5	6.9
G141	0.2850	0.0004	4.6215	0.0110	0.1113	0.0018	25.0	70.4	1.01	1616.2	5.1	1753.2	28.0	1821.4	28.5	11.3
G142	0.0282	0.0046	0.1994	0.2478	0.0516	0.0031	12.1	343.8	1.08	179.0	57.9	184.6	59.3	267.3	29.1	3.1
G143	0.0430	0.0043	0.3447	0.2372	0.0573	0.0032	16.8	334.2	0.83	271.2	53.9	300.7	59.5	502.3	44.3	9.8
G144	0.3415	0.0005	5.4128	0.0108	0.1153	0.0018	138.2	386.2	0.29	1893.7	5.0	1886.9	27.0	1883.8	26.9	-0.5
G145	0.1240	0.0007	1.2200	0.0180	0.0673	0.0018	13.7	86.8	1.16	753.3	8.3	809.8	29.5	847.1	30.6	7.0
G146	0.0697	0.0051	0.5324	0.2774	0.0562	0.0033	34.1	432.0	0.71	434.3	62.4	433.4	67.6	461.1	44.1	-0.2
G147	0.0648	0.0019	0.5199	0.0644	0.0564	0.0021	17.1	235.1	0.66	404.7	24.1	425.1	33.1	466.6	28.5	4.8
G148	0.3022	0.0011	4.7255	0.0279	0.1130	0.0017	98.1	321.9	0.21	1702.1	11.3	1771.8	26.9	1848.4	26.6	7.9
G149	0.2298	0.0010	2.9113	0.0281	0.0919	0.0019	114.2	478.5	0.33	1333.2	11.5	1384.8	32.4	1465.1	32.4	9.0
G150	0.0707	0.0046	0.5446	0.2455	0.0561	0.0034	42.0	546.1	0.56	440.3	56.1	441.5	64.1	456.7	44.6	0.3

Table 3
Summary of lithofacies, stratigraphy, emplacement process and depositional setting of the Tuen Mun Formation.

Lithofacies	Bedform	Emplacement Process	Depositional Setting
Tuen Mun Andesite Member			
Dominant lithofacies			
Andesite Lava	Massive lava flows up to xx m thick Figures 5E, 6G, 7E	Volcanic effusion	Subaerial stratovolcano
Autobreccia	Irregular, some basal to andesite lava flows, some possible hyaloclastite. Figure 6F	Volcanic effusion	Subaerial stratovolcano to shallow subaqueous
Andesitic lapilli-bearing ash crystal tuff	Massive units, several metres thick. Figure 7F	Pyroclastic flow and fall	Subaerial stratovolcano
Subordinate lithofacies			
Crystal-rich volcaniclastic sandstone with andesitic composition	Massive units, several metres thick.	Syn-eruptive high density gravity flows	Shallow subaqueous
Andesite-sandstone peperite	Massive units, several metres thick	Andesite dyke/sill intrusion into wet, unconsolidated sediments	Shallow subaqueous volcano
Siu Hang Tsuen Member			
Dominant lithofacies			
Polymictic, tuffaceous conglomerate/ sandstone/siltstone with or without marble clasts	Massive, to normally graded units, several metres thick, subrounded to rounded clasts. Figure 5D	Subaerial, fluvial and debris flow deposits, ± suspension sediments	Subaerial volcano ring plain
Polymictic, conglomerate /sand-stone/siltstone with or without marble clasts	Massive, to cross-bedded units, several metres thick, interbedded with thinly laminated units. Figures 5A-B, 6F, 7C	Subaerial to subaqueous debris flow deposits, ± suspension sediments	Subaerial fluvial to shallow subaqueous
Subordinate lithofacies			
Polymictic, andesite-conglomerate peperite, with or without marble clasts	Massive, to normally graded units, up to xx m thick, interbedded with thinly laminated units. Figure 5C	Subaqueous debris flow deposits, ± suspension sediments	Shallow subaqueous
Andesite-sandstone peperite	Massive units, up to several metres thick. Figure 6E	Andesite dyke/sill intrusion into wet, unconsolidated sediments	Shallow subaqueous volcano
Tin Shui Wai Member			
Dominant lithofacies			
Monomictic, marble clast-bearing, tuffaceous breccia/sandstone/ siltstone	Massive units up to xx thick. Figures 6A, D	high-density turbidity currents or subaqueous debris flows, ± suspension sediments	Shallow marine, below wave-base
Monomictic, marble clast-bearing breccia/sandstone/ siltstone	Massive units, up to xx thick. Figure 6C, 7D	high-density turbidity currents or subaqueous debris flows, ± suspension sediments	Shallow marine, below wave-base
Marble Breccia	Massive units, up to 9 m thick. Figures 6D. 7A	Subaqueous debris flows	Shallow marine, below wave-base
Subordinate lithofacies			
Monomictic, andesite-breccia peperite	Massive units, up to xx m thick	Syn-eruptive high density gravity flows	Shallow marine, below wave-base, volcano
Andesite-sandstone peperite	Massive units, up to xx thick. Figure 6B	Andesite dyke/sill intrusion into wet, unconsolidated sediments	Mainly shallow marine, below wave base, volcano